Chapter 2

Synthesis of Nanomaterials

2.1 Introduction to Nanoparticle Synthesis[1]

The fabrication of nanomaterials with strict control over size, shape, and crystalline structure has inspired the application of nanochemistry to numerous fields including catalysis, medicine, and electronics. The use of nanomaterials in such applications also requires the development of methods for nanoparticle assembly or dispersion in various media. A majority of studies have been aimed at dispersion in aqueous media aimed at their use in medical applications and studies of environmental effects, however, the principles of nanoparticle fabrication and functionalization of nanoparticles transcends their eventual application. Herein, we review the most general routes to nanoparticles of the key types that may have particular application within the oil and gas industry for sensor, composite, or device applications.

Synthesis methods for nanoparticles are typically grouped into two categories: "top-down" and "bottom-up". The first involves division of a massive solid into smaller portions. This approach may involve milling or attrition, chemical methods, and volatilization of a solid followed by condensation of the volatilized components. The second, "bottom-up", method of nanoparticle fabrication involves condensation of atoms or molecular entities in a gas phase or in solution. The latter approach is far more popular in the synthesis of nanoparticles.

Dispersions of nanoparticles are intrinsically thermodynamically metastable, primarily due to their very high surface area, which represents a positive contribution to the free enthalpy of the system. If the activation energies are not sufficiently high, evolution of the nanoparticle dispersion occurs causing an increase in nanoparticle size as typified by an Ostwald ripening process. Thus, highly dispersed nanoparticles are only kinetically stabilized and cannot be prepared under conditions that exceed some threshold, meaning that so-called "soft-chemical" or "*chemie duce*" methods are preferred. In addition, the use of surface stabilization is employed in many nanomaterials to hinder sintering, recrystallization and aggregation.

2.1.1 Bibliography

- J. Gopalakrishnan, *Chem. Mater.*, 1995, **7**, 1265.

2.2 Carbon Nanomaterials[2]

2.2.1 Introduction

Although nanomaterials had been known for many years prior to the report of C_{60} the field of nanoscale science was undoubtedly founded upon this seminal discovery. Part of the reason for this explosion in

---

[1]This content is available online at <http://cnx.org/content/m22372/1.2/>.
[2]This content is available online at <http://cnx.org/content/m22580/1.4/>.

nanochemistry is that while carbon materials range from well-defined nano sized molecules (i.e., C_{60}) to tubes with lengths of hundreds of microns, they do not exhibit the instabilities of other nanomaterials as a result of the very high activation barriers to their structural rearrangement. As a consequence they are highly stable even in their unfunctionalized forms. Despite this range of carbon nanomaterials possible they exhibit common reaction chemistry: that of organic chemistry.

The previously unknown allotrope of carbon: C_{60}, was discovered in 1985, and in 1996, Curl, Kroto, and Smalley were awarded the Nobel Prize in Chemistry for the discovery. The other allotropes of carbon are graphite (sp^2) and diamond (sp^3). C_{60}, commonly known as the "buckyball" or "Buckminsterfullerene", has a spherical shape comprising of highly pyramidalized sp^2 carbon atoms. The C_{60} variant is often compared to the typical soccer football, hence buckyball. However, confusingly, this term is commonly used for higher derivatives. Fullerenes are similar in sheet structure to graphite but they contain pentagonal (or sometimes heptagonal) rings that prevent the sheet from being planar. The unusual structure of C_{60} led to the introduction of a new class of molecules known as fullerenes, which now constitute the third allotrope of carbon. Fullerenes are commonly defined as "any of a class of closed hollow aromatic carbon compounds that are made up of twelve pentagonal and differing numbers of hexagonal faces."

The number of carbon atoms in a fullerene range from C_{60} to C_{70}, C_{76}, and higher. Higher order fullerenes include carbon nanotubes that can be described as fullerenes that have been stretched along a rotational axis to form a tube. As a consequence of differences in the chemistry of fullerenes such as C_{60} and C_{70} as compared to nanotubes, these will be dealt with separately herein. In addition there have also been reports of nanohorns and nanofibers, however, these may be considered as variations on the general theme. It should be noted that fullerenes and nanotubes have been shown to be in flames produced by hydrocarbon combustion. Unfortunately, these naturally occurring varieties can be highly irregular in size and quality, as well as being formed in mixtures, making them unsuitable for both research and industrial applications.

2.2.2 Fullerenes

Carbon-60 (C_{60}) is probably the most studied individual type of nanomaterial. The spherical shape of C_{60} is constructed from twelve pentagons and twenty hexagons and resembles a soccer ball (Figure 2.1a). The next stable higher fullerene is C_{70} (Figure 2.1b) that is shaped like a rugby or American football. The progression of higher fullerenes continues in the sequence C_{74}, C_{76}, C_{78}, etc. The structural relationship between each involves the addition of six membered rings. Mathematically (and chemically) two principles define the existence of a stable fullerene, i.e., Euler's theorem and isolated pentagon rule (IPR). Euler's theorem states that for the closure of each spherical network, n ($n \geq 2$) hexagons and 12 pentagons are required while the IPR says no two pentagons may be connected directly with each other as destabilization is caused by two adjacent pentagons.

(a)   (b)
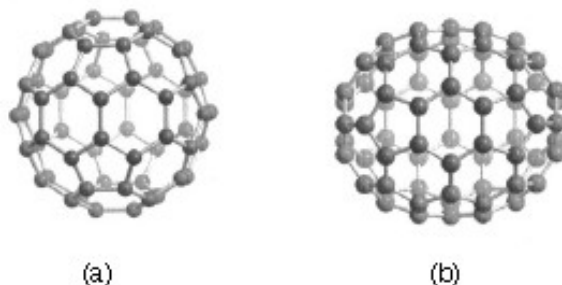
Figure 2.1: Molecular structures of (a) C_{60} and (b) C_{70}.

Although fullerenes are composed of sp^2 carbons in a similar manner to graphite, fullerenes are soluble in various common organic solvents. Due to their hydrophobic nature, fullerenes are most soluble in CS_2 (C_{60} = 7.9 mg/mL) and toluene (C_{60} = 2.8 mg/mL). Although fullerenes have a conjugated system, their aromaticity is distinctive from benzene that has all C-C bonds of equal lengths, in fullerenes two distinct classes of bonds exist. The shorter bonds are at the junctions of two hexagons ([6, 6] bonds) and the longer bonds at the junctions of a hexagon and a pentagon ([5,6] bonds). This difference in bonding is responsible for some of the observed reactivity of fullerenes.

2.2.2.1 Synthesis of fullerenes

The first observation of fullerenes was in molecular beam experiments at Rice University. Subsequent studies demonstrated that C_{60} it was relatively easy to produce grams of fullerenes. Although the synthesis is relatively straightforward fullerene purification remains a challenge and determines fullerene's commercial price. The first method of production of measurable quantities of fullerenes used laser vaporization of carbon in an inert atmosphere, but this produced microscopic amounts of fullerenes. Laboratory scales of fullerene are prepared by the vaporization of carbon rods in a helium atmosphere. Commercial production ordinarily employs a simple ac or dc arc. The fullerenes in the black soot collected are extracted in toluene and purified by liquid chromatography. The magenta C_{60} comes off the column first, followed by the red C_{70}, and other higher fullerenes. Even though the mechanism of a carbon arc differs from that of a resistively heated carbon rod (because it involves a plasma) the He pressure for optimum C_{60} formation is very similar.

A ratio between the mass of fullerenes and the total mass of carbon soot defines fullerene yield. The yields determined by UV-Vis absorption are approximately 40%, 10-15%, and 15% in laser, electric arc, and solar processes. Interestingly, the laser ablation technique has both the highest yield and the lowest productivity and, therefore, a scale-up to a higher power is costly. Thus, fullerene commercial production is a challenging task. The world's first computer controlled fullerene production plant is now operational at the MER Corporation, who pioneered the first commercial production of fullerene and fullerene products.

2.2.2.2 Endohedral fullerenes

Endohedral fullerenes are fullerenes that have incorporated in their inner sphere atoms, ions or clusters. Endohedral fullerenes are generally divided into two groups: endohedral metallofullerenes and non-metal doped fullerenes. The first endohedral metallofullerenes was called La@C_{60}. The @ sign in the name reflects the notion of a small molecule trapped inside a shell.

Doping fullerenes with metals takes place *in-situ* during the fullerene synthesis in an arc reactor or via laser evaporation. A wide range of metals have been encased inside a fullerene, i.e., Sc, Y, La, Ce, Ba, Sr, K, U, Zr, and Hf. Unfortunately, the synthesis of endohedral metallofullerenes is unspecific because in addition a high yield of unfilled fullerenes, compounds with different cage sizes are prepared (e.g., La@C_{60} or La@C_{82}). A characteristic of endohedral metallofullerenes is that electrons will transfer from the metal atom to the fullerene cage and that the metal atom takes a position off-center in the cage. The size of the charge transfer is not always simple to determine, but it is usually between 2 and 3 units (e.g., La$_2$@C_{80}) but can be as high as 6 electrons (e.g., Sc$_3$N@C_{80}). These anionic fullerene cages are very stable molecules and do not have the reactivity associated with ordinary empty fullerenes (see below). This lack of reactivity is utilized in a method to purify endohedral metallofullerenes from empty fullerenes.

The endohedral He@C_{60} and Ne@C_{60} form when C_{60} is exposed to a pressure of around 3 bar of the appropriate noble gases. Under these conditions it was possible to dope 1 in every 650,000 C_{60} cages with a helium atom. Endohedral complexes with He, Ne, Ar, Kr and Xe as well as numerous adducts of the He@C_{60} compound have also been proven with operating pressures of 3000 bars and incorporation of up to 0.1 % of the noble gases. The isolation of N@C_{60}, N@C_{70} and P@C_{60} is very unusual and unlike the metal derivatives no charge transfer of the pnictide atom in the center to the carbon atoms of the cage takes place.

2.2.2.3 Chemically functionalized fullerenes

Although fullerenes have a conjugated aromatic system all the carbons are quaternary (i.e., containing no hydrogen), which results in making many of the characteristic substitution reactions of planar aromatics impossible. Thus, only two types of chemical transformations exist: redox reactions and addition reactions. Of these, addition reactions have the largest synthetic value. Another remarkable feature of fullerene addition chemistry is the thermodymics of the process. Since the sp^2 carbon atoms in a fullerene are paramidalized there is significant strain energy. For example, the strain energy in C_{60} is *ca* 8 kcal/mol, which is 80% of its heat of formation. So the relief of this strain energy leading to sp^3 hybridized C atoms is the major driving force for addition reactions (Figure 2.2). As a consequence, most additions to fullerenes are exothermic reactions.
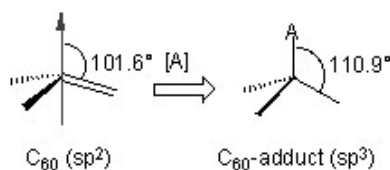
Figure 2.2: Strain release after addition of reagent A to a pyramidalize carbon of C_{60}.

Cyclic voltammetry (CV) studies show that C_{60} can be reduced and oxidized reversibly up to 6 electrons with one-electron transfer processes. Fulleride anions can be generated by electrochemical method and then be used to synthesize covalent organofullerene derivatives. Alkali metals can chemically reduce fullerene in solution and solid state to form $M_x C_{60}$ (x = 3 - 6). C_{60} can also be reduced by less electropositive metals like mercury to form C_{60}^- and C_{60}^{2-}. In addition, salts can also be synthesized with organic molecules, for example $[TDAE^+][C_{60}^-]$ possesses interesting electronic and magnetic behavior.

Geometric and electronic analysis predicted that fullerene behaves live an electro-poor conjugated polyolefin. Indeed C_{60} and C_{70} undergo a range of nucleophilic reactions with carbon, nitrogen, phosphorous and oxygen nucleophiles. C60 reacts readily with organolithium and Grignard compounds to form alkyl, phenyl or alkanyl fullerenes. Possibly the most widely used additions to fullerene is the Bingel reaction (Figure 2.3), where a carbon nucleophile, generated by deprotonation of α-halo malonate esters or ketones, is added to form a cyclopropanation product. The α-halo esters and ketones can also be generated in situ with I_2 or CBr_4 and a weak base as 1,8-diazabicyclo[5.4.0]unde-7ene (DBU). The Bingel reaction is considered one of the most versatile and efficient methods to functionalize C_{60}.
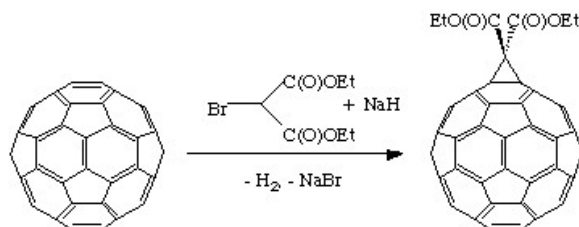
Figure 2.3: Bingel reaction of C_{60} with 2-bromoethylmalonate.

Cycloaddition is another powerful tool to functionalize fullerenes, in particular because of its selectivity with the 6,6 bonds, limiting the possible isomers (Figure 2.4). The dienophilic feature of the [6,6] double bonds of C_{60} enables the molecule to undergo various cycloaddition reactions in which the monoadducts can be generated in high yields. The best studies cycloadditon reactions of fullerene are [3+2] additions with diazoderivatives and azomethine ylides (Prato reactions). In this reaction, azomethine ylides can be generated *in situ* from condensation of α-amino acids with aldehydes or ketones, which produce 1,3 dipoles to further react with C_{60} in good yields (Figure 2.5). Hundreds of useful building blocks have been generated by those two methods. The Prato reactions have also been successfully applied to carbon nanotubes.
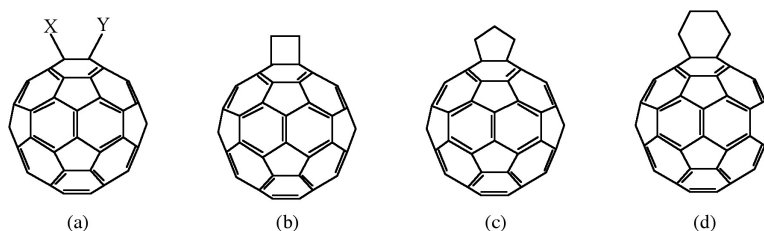
Figure 2.4: Geometrical shapes built onto a [6,6] ring junction: a) open, b) four-membered ring, c) five-membered ring, and d) six-membered ring.
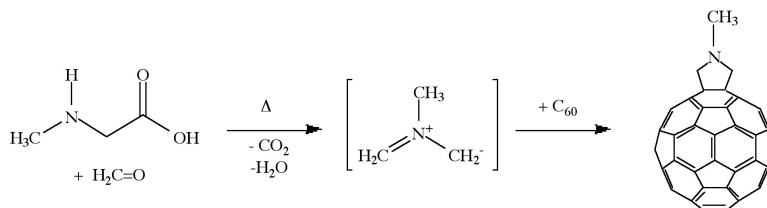
Figure 2.5: Prato reaction of C_{60} with N-methyglycine and paraformaldehyde.

The oxidation of fullerenes, such as C_{60}, has been of increasing interest with regard to applications in photoelectric devices, biological systems, and possible remediation of fullerenes. The oxidation of C_{60} to $C_{60}O_n$ (n = 1, 2) may be accomplished by photooxidation, ozonolysis, and epoxidation. With each of these methods, there is a limit to the isolable oxygenated product, $C_{60}O_n$ with n < 3. Highly oxygenated fullerenes, $C_{60}O_n$ with $3 \leq n \leq 9$, have been prepared by the catalytic oxidation of C_{60} with $ReMeO_3/H_2O_2$.

2.2.3 Carbon nanotubes

A key breakthrough in carbon nanochemistry came in 1993 with the report of needle-like tubes made exclusively of carbon. This material became known as carbon nanotubes (CNTs). There are several types of nanotubes. The first discovery was of multi walled tubes (MWNTs) resembling many pipes nested within each other. Shortly after MWNTs were discovered single walled nanotubes (SWNTs) were observed. Single walled tubes resemble a single pipe that is potentially capped at each end. The properties of single walled

and multi walled tubes are generally the same, although single walled tubes are believed to have superior mechanical strength and thermal and electrical conductivity; it is also more difficult to manufacture them.

Single walled carbon nanotubes (SWNTs) are by definition fullerene materials. Their structure consists of a graphene sheet rolled into a tube and capped by half a fullerene (Figure 2.6). The carbon atoms in a SWNT, like those in a fullerene, are sp2 hybridized. The structure of a nanotube is analogous to taking this graphene sheet and rolling it into a seamless cylinder. The different types of SWNTs are defined by their diameter and chirality. Most of the presently used single-wall carbon nanotubes have been synthesized by the pulsed laser vaporization method, however, increasingly SWNTs are prepared by vapor liquid solid catalyzed growth.
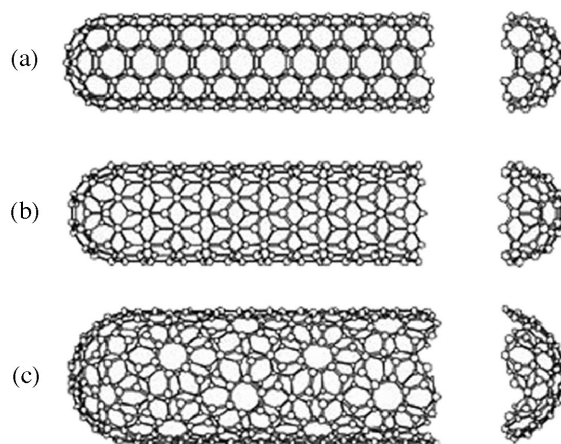
Figure 2.6: Structure of single walled carbon nanotubes (SWNTs) with (a) armchair, (b) zig-zag, and (c) chiral chirality.

The physical properties of SWNTs have made them an extremely attractive material for the manufacturing of nano devices. SWNTs have been shown to be stronger than steel as estimates for the Young's modulus approaches 1 Tpa. Their electrical conductance is comparable to copper with anticipate current densities of up to 10^{13} A/cm^2 and a resistivity as low as 0.34 x 10^{-4} Ω.cm at room temperatures. Finally, they have a high thermal conductivity (3000 - 6000 W.m/K).

The electronic properties of a particular SWNT structure are based on its chirality or twist in the structure of the tube which is defined by its n,m value. The values of n and m determine the chirality, or "twist" of the nanotube. The chirality in turn affects the conductance of the nanotube, its density, its lattice structure, and other properties. A SWNT is considered metallic if the value n-m is divisible by three. Otherwise, the nanotube is semi-conducting. The external environment also has an effect on the conductance of a tube, thus molecules such as O_2 and NH_3 can change the overall conductance of a tube, while the presence of metals have been shown to significantly effect the opto-electronic properties of SWNTs.

Multi walled carbon nanotubes (MWNTs) range from double walled NTs, through many-walled NTs (Figure 2.7) to carbon nanofibers. Carbon nanofibers are the extreme of multi walled tubes (Figure 2.8) and they are thicker and longer than either SWNTs or MWNTs, having a cross-sectional of ca. 500 Å^2 and are between 10 to 100 μm in length. They have been used extensively in the construction of high strength composites.
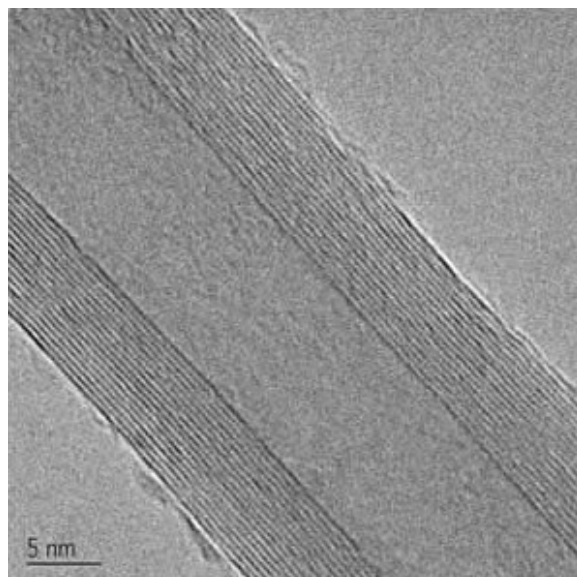
Figure 2.7: TEM image of an individual multi walled carbon nanotube (MWNTs). Copyright of Nanotech Innovations.
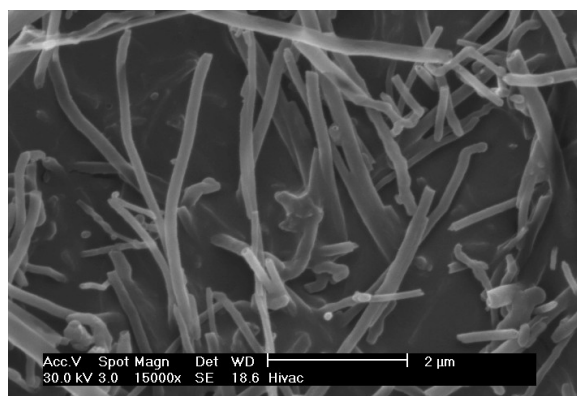
Figure 2.8: SEM image of vapor grown carbon nanofibers.

2.2.3.1 Synthesis of carbon nanotubes

A range of methodologies have been developed to produce nanotubes in sizeable quantities, including arc discharge, laser ablation, high pressure carbon monoxide (HiPco), and vapor liquid solid (VLS) growth. All

these processes take place in vacuum or at low pressure with a process gases, although VLS growth can take place at atmospheric pressure. Large quantities of nanotubes can be synthesized by these methods; advances in catalysis and continuous growth processes are making SWNTs more commercially viable.

The first observation of nanotubes was in the carbon soot formed during the arc discharge production of fullerenes. The high temperatures caused by the discharge caused the carbon contained in the negative electrode to sublime and the CNTs are deposited on the opposing electrode. Tubes produced by this method were initially multi walled tubes (MWNTs). However, with the addition of cobalt to the vaporized carbon, it is possible to grow single walled nanotubes. This method it produces a mixture of components, and requires further purification to separate the CNTs from the soot and the residual catalytic metals. Producing CNTs in high yield depends on the uniformity of the plasma arc, and the temperature of the deposit forming on the carbon electrode.

Higher yield and purity of SWNTs may be prepared by the use of a dual-pulsed laser. SWNTs can be grown in a 50% yield through direct vaporization of a Co/Ni doped graphite rod with a high-powered laser in a tube furnace operating at 1200 °C. The material produced by this method appears as a mat of "ropes", 10 - 20 nm in diameter and up to 100 μm or more in length. Each rope consists of a bundle of SWNTs, aligned along a common axis. By varying the process parameters such as catalyst composition and the growth temperature, the average nanotube diameter and size distribution can be varied. Although arc-discharge and laser vaporization are currently the principal methods for obtaining small quantities of high quality SWNTs, both methods suffer from drawbacks. The first is that they involve evaporating the carbon source, making scale-up on an industrial level difficult and energetically expensive. The second issue relates to the fact that vaporization methods grow SWNTs in highly tangled forms, mixed with unwanted forms of carbon and/or metal species. The SWNTs thus produced are difficult to purify, manipulate, and assemble for building nanotube-device architectures for practical applications.

In order to overcome some of the difficulties of these high-energy processes, the chemical catalysis method was developed in which a hydrocarbon feedstock is used in combination with a metal catalyst. The catalyst is typically, but not limited to iron, colbalt, or iron/molybdenum, it is heated under reducing conditions in the presence of a suitable carbon feedstock, e.g., ethylene. This method can be used for both SWNTs and MWNTs; the formation of each is controlled by the identity of the catalyst and the reaction conditions. A convenient laboratory scale apparatus is available from Nanotech Innovations, Inc., for the synthesis of highly uniform, consistent, research sample that uses pre-weighed catalyst/carbon source ampoules. This system, allows for 200 mg samples of MWNTs to be prepared for research and testing. The use of CO as a feedstock, in place of a hydrocarbon, led to the development of the high-pressure carbon monoxide (HiPco) procedure for SWNT synthesis. By this method, it is possible to produce gram quantities of SWNTs, unfortunately, efforts to scale beyond that have not met with complete success.

Initially developed for small-scale investigations of catalyst activity, vapor liquid solid (VLS) growth of nanotubes has been highly studied, and now shows promise for large-scale production of nanotubes. Recent approaches have involved the use of well-defined nanoparticle or molecular precursors and many different transition metals have been employed, but iron, nickel, and cobalt remain to be the focus of most research. The nanotubes grow at the sites of the metal catalyst; the carbon-containing gas is broken apart at the surface of the catalyst particle, and the carbon is transported to the edges of the particle, where it forms the nanotube. The length of the tube grown in surface supported catalyst VLS systems appears to be dependent on the orientation of the growing tube with the surface. By properly adjusting the surface concentration and aggregation of the catalyst particles it is possible to synthesize vertically aligned carbon nanotubes, i.e., as a carpet perpendicular to the substrate.

Of the various means for nanotube synthesis, the chemical processes show the greatest promise for industrial scale deposition in terms of its price/unit ratio. There are additional advantages to the VLS growth, which unlike the other methods is capable of growing nanotubes directly on a desired substrate. The growth sites are controllable by careful deposition of the catalyst. Additionally, no other growth methods have been developed to produce vertically aligned SWNTs.

2.2.3.2 Chemical functionalization of carbon nanotubes

The limitation of using carbon nanotubes in any practical applications has been its solubility; for example SWNTs have little to no solubility in most solvent due to the aggregation of the tubes. Aggregation/roping of nanotubes occurs as a result of the high van der Waals binding energy of *ca.* 500 eV per mm of tube contact. The van der Waals force between the tubes is so great, that it take tremendous energy to pry them apart, making it very to make combination of nanotubes with other materials such as in composite applications. The functionalization of nanotubes, i.e., the attachment of "chemical functional groups" provides the path to overcome these barriers. Functionalization can improve solubility as well as processibility, and has been used to align the properties of nanotubes to those of other materials. The clearest example of this is the ability to solubilize nanotubes in a variety of solvents, including water. It is important when discussing functionalization that a distinction is made between covalent and non-covalent functionalization.

Current methods for solubilizing nanotubes without covalent functionalization include highly aromatic solvents, super acids, polymers, or surfactants. Non-covalent "functionalization" is generally on the concept of supramolecular interactions between the SWNT and some macromolecule as a result of various adsorption forces, such as van der Waals' and π-stacking interactions. The chemical speciation of the nanotube itself is not altered as a result of the interaction. In contrast, covalent functionalization relies on the chemical reaction at either the sidewall or end of the SWNT. As may be expected the high aspect ratio of nanotubes means that sidewall functionalization is much more important than the functionalization of the cap. Direct covalent sidewall functionalization is associated with a change of hybridization from sp^2 to sp^2 and a simultaneous loss of conjugation. An alternative approach to covalent functionalization involves the reaction of defects present (or generated) in the structure of the nanotube. Defect sites can be the open ends and holes in the sidewalls, and pentagon and heptagon irregularities in the hexagon graphene framework (often associated with bends in the tubes). All these functionalizations are exohedral derivatizations. Taking the hollow structure of nanotubes into consideration, endohedral functionalization of SWNTs is possible, i.e., the filling of the tubes with atoms or small molecules. It is important to note that covalent functionalization methods have one problem in common: extensive covalent functionalization modifies SWNT properties by disrupting the continuous π-system of SWNTs.

Various applications of nanotubes require different, specific modification to achieve desirable physical and chemical properties of nanotubes. In this regard, covalent functionalization provides a higher degree of fine-tuning the chemistry and physics of SWNTs than non-covalent functionalization. Until now, a variety of methods have been used to achieve the functionalization of nanotubes (Figure 2.9).
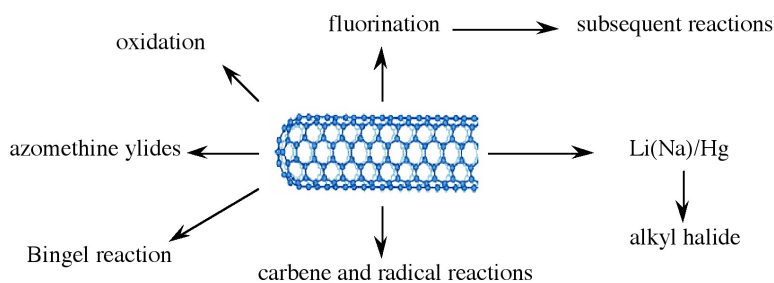
Figure 2.9: Schematic description of various covalent functionalization strategies for SWNTs.

Taking chemistry developed for C_{60}, SWNTs may be functionalized using 1,3 dipolar addition of azomethine ylides. The functionalized SWNTs are soluble in most common organic solvents. The azomethine ylide functionalization method was also used for the purification of SWNTs. Under electrochemical conditions, aryl

diazonium salts react with SWNTs to achieve functionalized SWNTs, alternatively the diazonium ions may be generated *in-situ* from the corresponding aniline, while a solvent free reaction provides the best chance for large-scale functionalization this way. In each of these methods it is possible to control the amount of functionalization on the tube by varying reaction times and the reagents used; functionalization as high as 1 group per every 10 - 25 carbon atoms is possible.

Organic functionalization through the use of alkyl halides, a radical pathway, on tubes treated with lithium in liquid ammonia offers a simple and flexible route to a range of functional groups. In this reaction, functionalization occurs on every 17 carbons. Most success has been found when the tubes are dodecylated. These tubes are soluble in chloroform, DMF, and THF.

The addition of oxygen moieties to SWNT sidewalls can be achieved by treatment with acid or wet air oxidation, and ozonolysis. The direct epoxidation of SWNTs may be accomplished by the direct reaction with a peroxide reagent, or catalytically. Catalytic de-epoxidation (Figure 2.10) allows for the quantitative analysis of sidewall epoxide and led to the surprising result that previously assumed "pure" SWNTs actually contain *ca.* 1 oxygen per 250 carbon atoms.
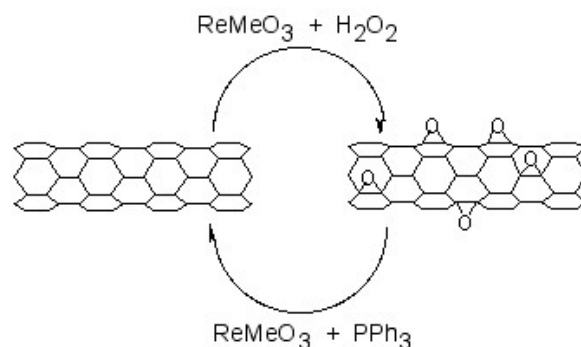
Figure 2.10: Catalytic oxidation and de-epoxidation of SWNTs.

One of the easiest functionalization routes, and a useful synthon for subsequent conversions, is the fluorination of SWNTs, using elemental fluorine. Importantly, a C:F ratios of up to 2:1 can be achieved without disruption of the tubular structure. The fluorinated SWNTs (F-SWNTs) proved to be much more soluble than pristine SWNTs in alcohols (1 mg/mL in *iso*-propanol), DMF and other selected organic solvents. Scanning tunneling microscopy (STM) revealed that the fluorine formed bands of approximately 20 nm, while calculations using DFT revealed 1,2 addition is more energetically preferable than 1,4 addition, which has been confirmed by solid state ^{13}C NMR. F-SWNTs make highly flexible synthons and subsequent elaboration has been performed with organo lithium, Grignard reagents, and amines.

Functionalized nanotubes can be characterized by a variety of techniques, such as atomic force microscopy (AFM), transmission electron microscopy (TEM), UV-vis spectroscopy, and Raman spectroscopy. Changes in the Raman spectrum of a nanotube sample can indicate if functionalization has occurred. Pristine tubes exhibit two distinct bands. They are the radial breathing mode (230 cm^{-1}) and the tangential mode (1590 cm^{-1}). When functionalized, a new band, called the disorder band, appears at *ca.*1350 cm^{-1}. This band is attributed to sp^3-hybridized carbons in the tube. Unfortunately, while the presence of a significant D mode is consistent with sidewall functionalization and the relative intensity of D (disorder) mode versus the tangential G mode (1550 − 1600 cm^{-1}) is often used as a measure of the level of substitution. However, it has been shown that Raman is an unreliable method for determination of the extent of functionalization since the relative intensity of the D band is also a function of the substituents distribution as well as concentration.

Recent studies suggest that solid state ^{13}C NMR are possibly the only definitive method of demonstrating covalent attachment of particular functional groups.

2.2.3.3 Coating carbon nanotubes: creating inorganic nanostructures

Fullerenes, nanotubes and nanofibers represent suitable substrates for the seeding other materials such as oxides and other minerals, as well as semiconductors. In this regard, the carbon nanomaterial acts as a seed point for the growth as well as a method of defining unusual aspect ratios. For example, silica fibers can be prepared by a number of methods, but it is only through coating SWNTs that silica nano-fibers with of micron lengths with tens of nanometers in diameter may be prepared.

While C_{60} itself does not readily seed the growth of inorganic materials, liquid phase deposition of oxides, such as silica, in the presence of fullerenol, $C_{60}(OH)_n$, results in the formation of uniform oxide spheres. It appears the fullerenol acts as both a reagent and a physical point for subsequent oxide growth, and it is C_{60}, or an aggregate of C_{60}, that is present within the spherical particle. The addition of fullerenol alters the morphology and crystal phase of $CaCO_3$ precipitates from aqueous solution, resulting in the formation of spherical features, 5-pointed flower shaped clusters, and triangular crystals as opposed to the usual rhombic crystals. In addition, the meta-stable vaterite phase is observed with the addition of $C_{60}(OH)_n$.

As noted above individual SWNTs may be obtained in solution when encased in a cylindrical micelle of a suitable surfactant. These individualized nanotubes can be coated with a range of inorganic materials. Liquid phase deposition (LPD) appears to have significant advantages over other methods such as incorporating surfaced SWNTs into a preceramic matrix, *in situ* growth of the SWNT in an oxide matrix, and sol-gel methods. The primary advantage of LPD growth is that individual SWNTs may be coated rather than bundles or ropes. For example, SWNTs have been coated with silica by liquid phase deposition (LPD) using a silica/H_2SiF_6 solution and a surfactant-stabilized solution of SWNTs. The thickness of the coating is dependent on the reaction mixture concentration and the reaction time. The SWNT core can be removed by thermolysis under oxidizing conditions to leave a silica nano fiber. It is interesting to note that the use of a surfactant is counter productive when using MWNTs and VGFs, in this case surface activation of the nanotube offers the suitable growth initiation. Pre-oxidation of the MWNT or VGF allows for uniform coatings to be deposited. The coated SWNTs, MWNTs, and VGFs can be subsequently reacted with suitable surface reagents to impart miscibility in aqueous solutions, guar gels, and organic matrixes. In addition to simple oxides, coated nanotubes have been prepared with minerals such as carbonates and semiconductors.

2.2.4 Bibliography

- S. M. Bachilo, M. S. Strano, C. Kittrell, R. H. Hauge, R. E. Smalley, and R. B. Weisman, *Science*, 2002, **298**, 2361.
- D. S. Bethune, C. H. Klang, M. S. deVries, G. Gorman, R. Savoy, J. Vazquez, and R. Beyers, *Nature*, 1993, **363**, 605.
- J, J. Brege, C. Gallaway, and A. R. Barron, *J. Phys. Chem., C*, 2007, **111**, 17812.
- C. A. Dyke and J. M. Tour, *J. Am. Chem. Soc.*, 2003, **125**, 1156.
- Z. Ge, J. C. Duchamp, T. Cai, H. W. Gibson, and H. C. Dorn, *J. Am. Chem. Soc.*, 2005, **127**, 16292.
- L. A. Girifalco, M. Hodak, and R. S. Lee, *Phys. Rev. B*, 2000, **62**, 13104.
- T. Guo, P. Nikolaev, A. G. Rinzler, D. Tománek, D. T. Colbert, and R. E. Smalley, *J. Phys. Chem.*, 1995, **99**, 10694.
- J. H. Hafner, M. J. Bronikowski, B. R. Azamian, P. Nikolaev, A. G. Rinzler, D. T. Colbert, K. A. Smith, and R. E. Smalley, *Chem. Phys. Lett.*, 1998, **296**, 195.
- A. Hirsch, *Angew. Chem. Int. Ed.*, 2002, **40**, 4002.
- S. Iijima and T. Ichihashi, *Nature*, 1993, **363**, 603.
- H. R. Jafry, E. A. Whitsitt, and A. R. Barron, *J. Mater. Sci.*, 2007, **42**, 7381.
- H. W. Kroto, J. R. Heath, S. C. O'Brien, R. F. Curl, and R. E. Smalley, *Nature*, 1985, **318**, 162.
- F. Liang, A. K. Sadana, A. Peera, J. Chattopadhyay, Z. Gu, R. H. Hauge, and W. E. Billups, *Nano Lett.*, 2004, **4**, 1257.

- D. Ogrin and A. R. Barron, *J. Mol. Cat. A: Chem.*, 2006, **244**, 267.
- D. Ogrin, J. Chattopadhyay, A. K. Sadana, E. Billups, and A. R. Barron, *J. Am. Chem. Soc.*, 2006, **128**, 11322.
- R. E. Smalley, *Acc. Chem. Res.*, 1992, **25**, 98.
- M. M. J. Treacy, T. W. Ebbesen, and J. M. Gibson, *Nature*, 1996, **381**, 678.
- E. A. Whitsitt and A. R. Barron, *Nano Lett.*, 2003, **3**, 775.
- J. Yang and A. R. Barron, *Chem. Commun.*, 2004, 2884.
- L. Zeng, L. B. Alemany, C. L. Edwards, and A. R. Barron, *Nano Res.*, 2008, **1**, 72.

2.3 Graphene[3]

2.3.1 Introduction

Graphene is a one-atom-thick planar sheet of sp^2-bonded carbon atoms that are densely packed in a honeycomb crystal lattice (Figure 2.11). The name comes from "graphite" and "alkene"; graphite itself consists of many graphene sheets stacked together.
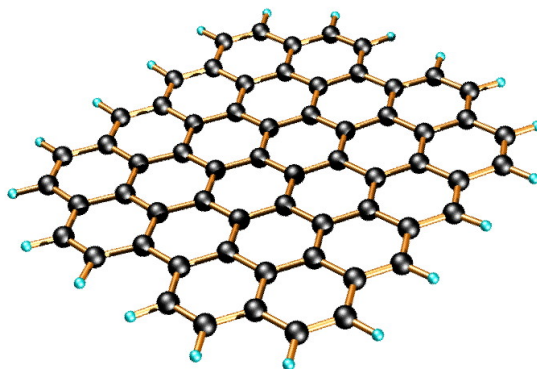
Figure 2.11: Idealized structure of a single graphene sheet.

Single-layer graphene nanosheets were first characterized in 2004, prepared by mechanical exfoliation (the "scotch-tape" method) of bulk graphite. Later graphene was produced by epitaxial chemical vapor deposition on silicon carbide and nickel substrates. Most recently, graphene nanoribbons (GNRs) have been prepared by the oxidative treatment of carbon nanotubes and by plasma etching of nanotubes embedded in polymer films.

2.3.2 Physical properties of graphene

Graphene has been reported to have a Young's modulus of 1 TPa and intrinsic strength of 130 GP; similar to single walled carbon nanotubes (SWNTs). The electronic properties of graphene also have some similarity with carbon nanotubes. Graphene is a zero-bandgap semiconductor. Electron mobility in graphene is extraordinarily high (15,000 cm^2/V.s at room temperature) and ballistic electron transport is reported to

[3]This content is available online at <http://cnx.org/content/m29187/1.4/>.

be on length scales comparable to that of SWNTs. One of the most promising aspects of graphene involves the use of GNRs. Cutting an individual graphene layer into a long strip can yield semiconducting materials where the bandgap is tuned by the width of the ribbon.

While graphene's novel electronic and physical properties guarantee this material will be studied for years to come, there are some fundamental obstacles yet to overcome before graphene based materials can be fully utilized. The aforementioned methods of graphene preparation are effective; however, they are impractical for large-scale manufacturing. The most plentiful and inexpensive source of graphene is bulk graphite. Chemical methods for exfoliation of graphene from graphite provide the most realistic and scalable approach to graphene materials.

Graphene layers are held together in graphite by enormous van der Waals forces. Overcoming these forces is the major obstacle to graphite exfoliation. To date, chemical efforts at graphite exfoliation have been focused primarily on intercalation, chemical derivatization, thermal expansion, oxidation-reduction, the use of surfactants, or some combination of these.

2.3.3 Graphite oxide

Probably the most common route to graphene involves the production of graphite oxide (GO) by extremely harsh oxidation chemistry. The methods of Staudenmeier or Hummers are most commonly used to produce GO, a highly exfoliated material that is dispersible in water. The structure of GO has been the subject of numerous studies; it is known to contain epoxide functional groups along the basal plane of sheets as well as hydroxyl and carboxyl moieties along the edges (Figure 2.12). In contrast to other methods for the synthesis of GO, the the m-peroxybenzoic acid (m-CPBA) oxidation of microcrystalline synthetic graphite at room temperature yields graphite epoxide in high yield, without significant additional defects.
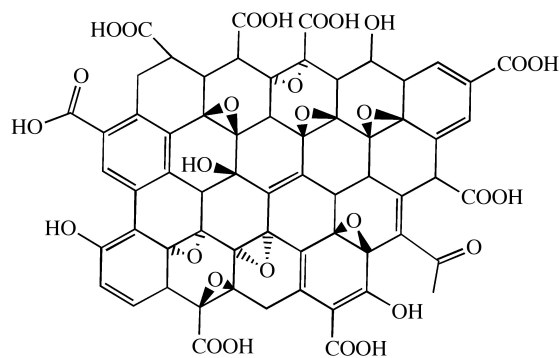
Figure 2.12: Idealized structure proposed for graphene oxide (GO). Adapted from C. E. Hamilton, PhD Thesis, Rice University (2009).

As graphite oxide is electrically insulating, it must be converted by chemical reduction to restore the electronic properties of graphene. Chemically converted graphene (CCG) is typically reduced by hydrazine or borohydride. The properties of CCG can never fully match those of graphene for two reasons:

1. Oxidation to GO introduces defects.
2. Chemical reduction does not fully restore the graphitic structure.

As would be expected, CCG is prone to aggregation unless stabilized. Graphene materials produced from pristine graphite avoid harsh oxidation to GO and subsequent (incomplete) reduction; thus, materials produced are potentially much better suited to electronics applications.

A catalytic approach to the removal of epoxides from fullerenes and SWNTs has been applied to graphene epoxide and GO. Treatment of oxidized graphenes with methyltrioxorhenium (MeReO$_3$, MTO) in the presence of PPh$_3$ results in the oxygen transfer, to form O=PPh$_3$ and allow for quantification of the C:O ratio.

2.3.4 Homogeneous graphene dispersions

An alternate approach to producing graphene materials involves the use of pristine graphite as starting material. The fundamental value of such an approach lies in its avoidance of oxidation to GO and subsequent (incomplete) reduction, thereby preserving the desirable electronic properties of graphene. There is precedent for exfoliation of pristine graphite in neat organic solvents without oxidation or surfactants. It has been reported that *N,N*-dimethylformamide (DMF) dispersions of graphene are possible, but no detailed characterization of the dispersions were reported. In contrast, Coleman and coworkers reported similar dispersions using *N*-methylpyrrolidone (NMP), resulting in individual sheets of graphene at a concentration of ≤0.01 mg/mL. NMP and DMF are highly polar solvents, and not ideal in cases where reaction chemistry requires a nonpolar medium. Further, they are hygroscopic, making their use problematic when water must be excluded from reaction mixtures. Finally, DMF is prone to thermal and chemical decomposition.

Recently, dispersions of graphene has been reported in *ortho*-dichlorobenzene (ODCB) using a wide range of graphite sources. The choice of ODCB for graphite exfoliation was based on several criteria:

1. ODCB is a common reaction solvent for fullerenes and is known to form stable SWNT dispersions.
2. ODCB is a convenient high-boiling aromatic, and is compatible with a variety of reaction chemistries.
3. ODCB, being aromatic, is able to interact with graphene *via* π-π stacking.
4. It has been suggested that good solvents for graphite exfoliation should have surface tension values of $40 - 50$ mJ/m^2. ODCB has a surface tension of 36.6 mJ/m^2, close to the proposed range.

Graphite is readily exfoliated in ODCB with homogenization and sonication. Three starting materials were successfully dispersed: microcrystalline synthetic, thermally expanded, and highly ordered pyrolytic graphite (HOPG). Dispersions of microcrystalline synthetic graphite have a concentration of 0.03 mg/mL, determined gravimetrically. Dispersions from expanded graphite and HOPG are less concentrated (0.02 mg/mL).

High resolution transmission electron microscopy (HRTEM) shows mostly few-layer graphene (n < 5) with single layers and small flakes stacked on top (Figure 2.13). Large graphitic domains are visible; this is further supported by selected area electron diffraction (SAED) and fast Fourier transform (FFT) in selected areas. Atomic force microscope (AFM) images of dispersions sprayed onto silicon substrates shows extremely thin flakes with nearly all below 10 nm. Average height is 7 - 10 nm. The thinnest are less than 1 nm, graphene monolayers. Lateral dimensions of nanosheets range from $100 - 500$ nm.
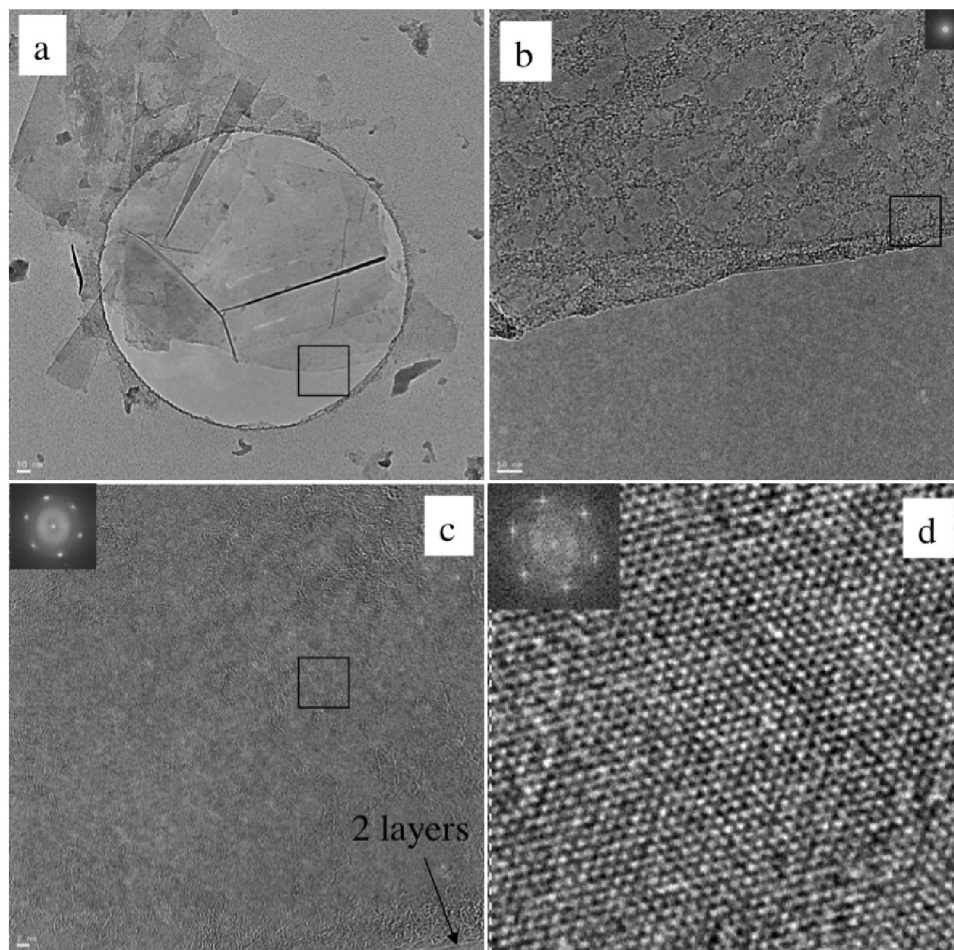
Figure 2.13: TEM images of single layer graphene from HOPG dispersion. (a) monolayer and few layer of graphene stacked with smaller flakes; (b) selected edge region from (a), (c) selected area from (b) with FFT inset, (d) HRTEM of boxed region in (c) showing lattice fringes with FFT inset. Adapted from C. E. Hamilton, PhD Thesis, Rice University (2009).

As-deposited films cast from ODCB graphene show poor electrical conductivity, however, after vacuum annealing at 400 °C for 12 hours the films improve vastly, having sheet resistances on the order of 60 Ω/sq. By comparison, graphene epitaxially grown on Ni has a reported sheet resistance of 280 Ω/sq.

2.3.5 Covalent functionalization of graphene and graphite oxide

The covalent functionalization of SWNTs is well established. Some routes to covalently functionalized SWNTs include esterification/ amidation, reductive alkylation (Billups reaction), and treatment with azomethine ylides (Prato reaction), diazonium salts, or nitrenes. Conversely, the chemical derivatization of graphene and GO is still relatively unexplored.

Some methods previously demonstrated for SWNTs have been adapted to GO or graphene. GO carboxylic acid groups have been converted into acyl chlorides followed by amidation with long-chain amines.

Additionally, the coupling of primary amines and amino acids via nucleophilic attack of GO epoxide groups has been reported. Yet another route coupled isocyanates to carboxylic acid groups of GO. Functionalization of partially reduced GO by aryldiazonium salts has also been demonstrated. The Billups reaction has been performed on the intercalation compound potassium graphite (C_8K), as well as graphite fluoride, and most recently GO. Graphene alkylation has been accomplished by treating graphite fluoride with alkyllithium reagents.

ODCB dispersions of graphene may be readily converted to covalently functionalize graphene. Thermal decomposition of benzoyl peroxide is used to initiate radical addition of alkyl iodides to graphene in ODCB dispersions.

$$(2.1)$$
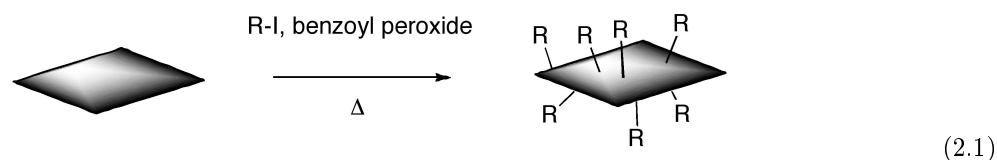
Additionally, functionalized graphene with nitrenes generated by thermal decomposition of aryl azides

$$(2.2)$$
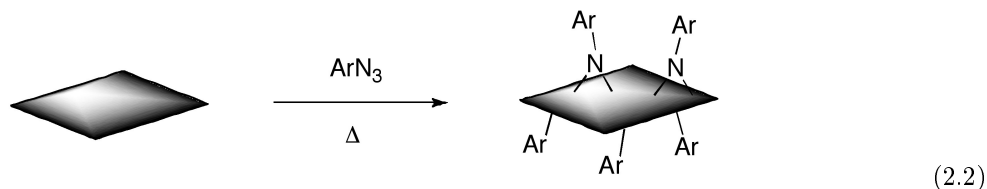
2.3.6 Bibliography

- P. Blake, P. D. Brimicombe, R. R. Nair, T. J. Booth, D. Jiang, F. Schedin, L. A. Ponomarenko, S. V. Morozov, H. F. Gleeson, E. W. Hill, A. K. Geim, and K. S. Novoselov, *Nano Lett.*, 2008, **8**, 1704.
- J. Chattopadhyay, A. Mukherjee, C. E. Hamilton, J.-H. Kang, S. Chakraborty, W. Guo, K. F. Kelly, A. R. Barron, and W. E. Billups, *J. Am. Chem. Soc.*, 2008, **130**, 5414.
- G. Eda, G. Fanchini, and M. Chhowalla, *Nat. Nanotechnol.*, 2008, **3**, 270.
- M. Y. Han, B. Ozyilmaz, Y. Zhang, and P. Kim, *Phys. Rev. Lett.*, 2008, **98**, 206805.
- Y. Hernandez, V. Nicolosi, M. Lotya, F. M. Blighe, Z. Sun, S. De, I. T. McGovern, B. Holland, M. Byrne, Y. K. Gun'Ko, J. J. Boland, P. Niraj, G. Duesberg, S. Krishnamurthy, R. Goodhue, J. Hutchinson, V. Scardaci, A. C. Ferrari, and J. N. Coleman, *Nat. Nanotechnol.*, 2008, **3**, 563.
- W. S. Hummers and R. E. Offeman, *J. Am. Chem. Soc.*, 1958, **80**, 1339.
- L. Jiao, L. Zhang, X. Wang, G. Diankov, and H. Dai, *Nature*, 2009, **458**, 877.
- D. V. Kosynkin, A. L. Higginbotham, A. Sinitskii, J. R. Lomeda, A. Dimiev, B. K. Price, and J. M. Tour, *Nature*, 2009, **458**, 872.
- D. Li, M. B. Mueller, S. Gilje, R. B. Kaner, and G. G. Wallace, *Nat. Nanotechnol.*, 2008, **3**, 101.
- S. Niyogi, E. Bekyarova, M. E. Itkis, J. L. McWilliams, M. A. Hamon, and R. C. Haddon, *J. Am. Chem. Soc.*, 2006, **128**, 7720.
- Y. Si and E. T. Samulski, *Nano Lett.*, 2008, **8**, 1679.
- L. Staudenmaier, *Ber. Dtsch. Chem. Ges.*, 1898, **31**, 1481.

2.4 Oxide Nanoparticles[4]

2.4.1 Introduction to oxide nanoparticles

The most widespread route to fabrication of metal oxide nanoparticles involves the "bottom-up" approach involving the precipitation from aqueous solution from metal salts. Organometallic species can also be used, but due to their cost and the difficulty in manipulating these compounds, they are used less frequently. An alternative "top-down" approach has been demonstrated for aluminum and iron oxide nanoparticles; however, it is possible that this methodology could be extended to other oxides.

2.4.2 From molecular species to nanoparticles

Hydroxide, oxyhydroxide or hydrated oxide solid phases obtained via precipitation are made of particles whose average size may range from a few nanometers to a few microns. Particle morphology may vary depending on synthesis conditions. Moreover, aging in aqueous solution may bring about significant dimensional, morphological and structural changes.

2.4.2.1 Use of metal salts

The dissolution of metal salts in water results in the formation of solvated coordination compounds in which the chemistry of such complexes, and especially their acid behavior, provides a framework for understanding how the solid (oxide) forms via polycondensation. The binding of water molecules to the metal cation results in the increase in the acidity such that they tend to be deprotonate spontaneously according to the hydrolysis equilibrium

$[M(H_2O)_n]^{z+} + h\ H_2O \rightarrow [M(OH)_h(H_2O)_{n-h}]^{(z-h)+} + h\ H_3O^+$
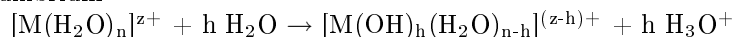
or by the neutralisation with a base,

$[M(H_2O)_n]^{z+} + h\ HO- \rightarrow [M(OH)_h(H_2O)_{n-h}]^{(z-h)+} + h\ H_2O$
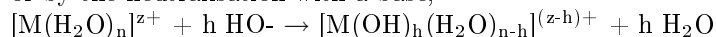
in which h is the hydroxylation ratio of the cation. The resulting hydroxylated complexes condense via two basic mechanisms of nucleophilic substitution, depending on the nature of the coordination sphere of the cations. Condensation of aquohydroxo complexes proceeds by elimination of water and formation of hydroxo bridges (olation), while for oxohydroxo complexes, condensation proceedes via the formation of oxo bridges (oxolation).

In order to understand how small particles form and what role the experimental parameters play on their characteristics and on evolution, it is useful to review the kinetic aspects of condensation reactions. The precipitation of a solid involves four kinetic steps.

 i. Formation of the zero-charge precursor. $[M(OH)_z(H_2O)_{n-z}]^0$, which is able to condense and form a solid phase.
 ii. Creation of nuclei, through condensation of zero-charge precursors.
 iii. Growth of the nuclei through addition of matter, until the primary particle stage is reached.
 iv. Nucleation and growth steps form particles under kinetic control following a reaction path of minimum activation energy under conditions imposed to the system (acidity, concentration, temperature), but the products are not necessarily thermodynamically stable.

Aging of the suspensions, which may take place over a long time scale (hours, days or months), allows the system to tend toward, or reach stability, and it is often associated with modifications of some physical or chemical characteristics of the particles.

2.4.2.2 Use of metallo-oragnic compounds

Metallo-organic compounds, and especially metal alkoxides, are used in so-called sol-gel chemistry of oxide nanomaterials. Metal alkoxides are also precursors of hybrid organic-inorganic materials, because such

---

[4]This content is available online at <http://cnx.org/content/m22969/1.2/>.

compounds can be used to introduce an organic part inside the mineral component. Sol-gel chemistry mainly involves hydrolysis and condensation reactions of alkoxides $M(OR)_n$ in solution in an alcohol ROH, schematically represented as follows.

$M(OR)_n + n\ H_2O \rightarrow M(OH)_n + n\ ROH \rightarrow MO_{n/2} + {}^n/_2\ H_2O$
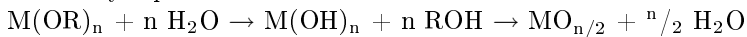
These reactions, hydroxylation and condensation, proceed by nucleophilic substitution of alkoxy or hydroxy ligands by hydroxylated species according to.

$M(OR)_n + x\ HOX \rightarrow [M(OR)_{n-x}(OX)_x] + n\ ROH$
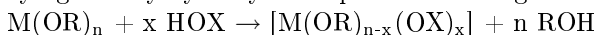
If X = H, the reaction is a hydroxylation. For X = M, it is a condensation and if X represents an organic or inorganic ligand, the reaction is a complexation. The reactivity of metal alkoxides towards hydrolysis and condensation is governed by three main parameters: the electrophilic character of the metal (its polarizing power), the steric effect of the alkoxy ligands and the molecular structure of the metal alkoxide. Generally, the reactivity of alkoxides towards substitutions increases when the electronegativity of the metal is low and its size is high. The reactivity of metal alkoxides is also very sensitive to the steric hindrance of the alkoxy groups. It strongly decreases when the size of the OR group increases. The acidity of the medium also influences the rate of hydrolysis and condensation reaction to a great extent as well as the morphology of the products.

2.4.2.3 Non-hydrolytic routes

Non hydrolytic sol-gel chemistry has proved to be a promising route to metal oxides, and it has become a widely explored approach to synthesize metal oxide nanoparticles under various conditions. These methods involve either the self-condensation of various metal compounds or the thermolysis of metal coordination compounds. However, since water may be produced by the thermolysis of the organic derivatives, a hydrolytic pathway cannot be excluded. One of the most studied approaches involves the thermolytic decomposition of an inorganic complex at high temperatures. Two approaches include: the decomposition of $Fe(acac)_3$ or $FeCl_3$ and $M(acac)_2$ salts, and the decomposition of $Fe(CO)_5$ and $M(acac)_2$ salts. For simple oxides (e.g., Fe_3O_4) the precursor, e.g., $Fe(acac)_3$, is added to a suitable solvent heated to a temperature that allows for the rapid decomposition of the precursor. The choice of temperature and the temperature control (i.e., variation of the temperature during the reaction) are important in defining the resulting nanoparticle size and size distribution. By this method highly uniform nanoparticles can be obtained (Figure 2.14).
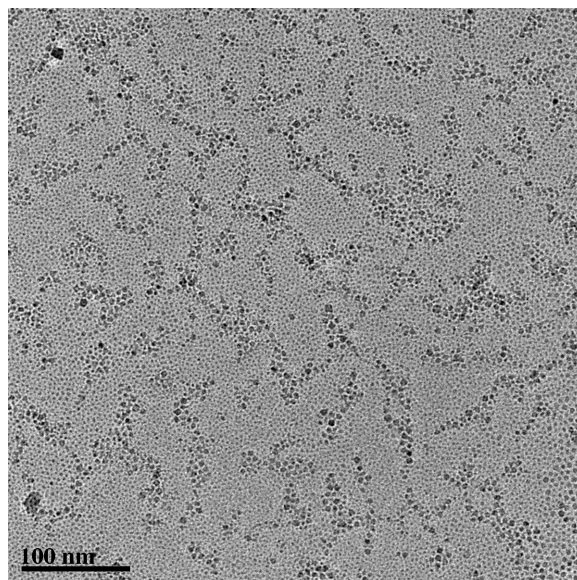
Figure 2.14: TEM image of 4 nm Fe_3O_4 nanoparticles prepared from the thermal decomposition of $Fe(acac)_3$.

In addition to simple metal oxides (M_xO_y) a range of mixed metal oxides can also be prepared. For example, nanospheres and nanocubes of cobalt ferrite can be obtained from cobalt and iron acetylacetonates, $Co(acac)_2$ and $Fe(acac)_3$ in solution in phenyl ether and hexadecanediol in the presence of oleic acid and oleylamine. Heating at 260 °C forms $CoFe_2O_4$ spherical nanocrystals with a diameter of 5 nm. These nanocrystals serve as seeds for a new growth as the second step of the synthesis, giving perfect nanocubes from 8 to 12 nm, depending on the conditions. Nanocubes in the 8 nm range can also be used as seeds to obtain spheres. The tuning of the shape of ferrite nanocrystals is managed by the parameters of growth such as heating rate, temperature, reaction time, ratio of seed to precursors, and ratio of oleic acid, acting as surfactant stabilizing the nanocrystal, to oleylamine providing basic conditions needed for the formation of spinel oxide.

Various morphologies of numerous oxide nanocrystals including Fe, Co, Mn ferrites, Co_3O_4, Cr_2O_3, MnO, NiO, ZnO, and others have been obtained by pyrolysis of metal carboxylates in the presence of different fatty acids (oleic, myristic). Control over the chemical composition of the nanoparticle is readily attained through the relative concentration of reagents used for nanoparticle growth. In many systems there is a direct linear relationship between the relative composition in the nano particles and the reagent solutions used.

2.4.3 From minerals to materials

As described above the "bottom-up" approach of reacting small inorganic molecules to form oligomeric and polymeric materials and subsequently nano particles is a common approach for a wide range of metal and non-metal oxides. However, in the case of aluminum oxide nanoparticles, the relative rate of the hydrolysis and condensation reactions often makes particle size control difficult. Once the structure of alumina sol-gels (known as alumoxanes) had been determined to comprise of a boehmite-like nanoparticle core, it was proposed that alumina nanoparticles could be prepared directly from the mineral. Such a "top-down" approach represented a departure from the traditional synthetic methodologies. Thus, it has been shown that

carboxylic acids (RCO_2H) react with boehmite, $[Al(O)(OH)]_n$, to yield the appropriate carboxy-alumoxane.

$$[Al(O)(OH)]_n + HO_2CR \rightarrow [Al(O)_x(OH)_y(O_2CR)_z]_n$$
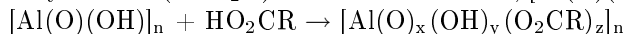
Initial syntheses were carried out using the acid as the solvent or xylene, however, subsequent research demonstrated the use of water as a solvent and acetic acid as the most convenient capping agent. A solventless synthesis has also been developed. Thus, the synthesis of alumoxane nanoparticles may be summarized as involving the reaction between dirt (boehmite), vinegar (acetic acid), and water. The function of the acid is two-fold. First, to cleave the mineral lattice and "carve out" nanoscale fragment, and second to provide a chemical cap to the fragment (Figure 2.15).
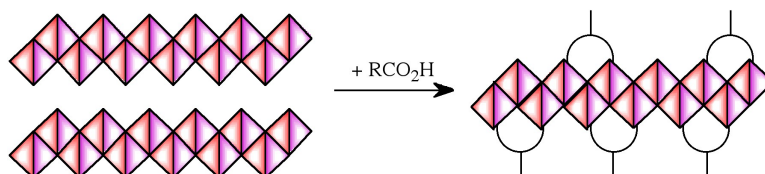
Figure 2.15: Pictorial representation of the reaction of boehmite with carboxylic acids.

The carboxylate-alumoxane nanoparticles prepared from the reaction of boehmite and carboxylic acids are air and water stable. The soluble carboxylate-alumoxanes can be dip-coated, spin coated, and spray-coated onto various substrates. The size of the alumoxane nanoparticles is dependant on the substituents, the reaction conditions (concentration, temperature, time, etc.), and the pH of the reaction solution. Unlike other forms of oxide nanoparticle, the alumoxanes are not mono-dispersed but have a range of particle sizes. Also unlike other metal oxide nanoparticles, the core of the alumoxane can undergo a low temperature reaction that allows for the incorporation of other metals (e.g., Ti, La, Mo, V, Ca). This occurs by reaction of metal acetylacetenoates $[M(acac)_n]$ with the carboxylate alumoxane (Figure 2.16).
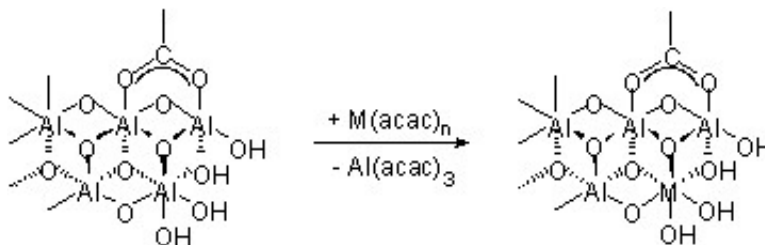
Figure 2.16: Schematic representation of the exchange reaction that occurs between a metal complex and the core of the alumoxane nanoparticle.

Given the analogous structure of $Fe(O)(OH)$ (lepidocrocite) to boehmite, it is not surprising that the iron analog of alumoxane nanoparticles (i.e., ferroxanes) is readily prepared. Ferroxanes have been extensively characterized, and have shown to have identical structural features to alumoxanes and undergo similar exchange reactions.

2.4.4 Bibliography

- A. W. Apblett, A. C. Warren, and A. R. Barron, *Chem. Mater.* , 1992, **4**, 167.
- R. L. Callender and A. R. Barron, *J. Am. Ceram. Soc.* , 2000, **83**, 1777.
- R. L. Callender, C. J. Harlan, N. M. Shapiro, C. D. Jones, D. L. Callahan, M. R. Wiesner, R. Cook, and A. R. Barron, *Chem. Mater.* , 1997, **9**, 2418.
- C. Crouse and A. R. Barron, *J. Mater. Chem.* , 2008, **18**, 4146.
- S. Han, T. Yu, J. Park, B. Koo, J. Joo, T. Hyeon, S. Hong, and J. Im, *J. Phys. Chem. B* , 2004, **108**, 8091.
- J. Rose, M. M. Cortalezzi-Fidalgo, S. Moustier, C. Magnetto, C. D. Jones, A. R. Barron, M. R. Wiesner, and J. Y. Bottero, *Chem. Mater.* , 2002, **14**, 621.
- N. Shahid and A. R. Barron, *J. Mater. Chem.* , 2004, **14**, 1235. Y. W. Jun, J. S. Choi, and J. Cheon, *Angew. Chem. Int. Ed.* , 2006, **45**, 2.
- A. Vioux, *Chem. Mater.*, 1997, **9**, 2292.

2.5 Synthesis of Magnetite Nanoparticles[5]

Numerous schemes have been devised to synthesize magnetite nanoparticles (nMag). The different methods of nMag synthesis can be generally grouped as aqueous or non-aqueous according to the solvents used. Two of the most widely used and explored methods for nMag synthesis are the aqueous co-precipitation method and the non-aqueous thermal decomposition method.

The co-precipitation method of nMag synthesis consists of precipitation of Fe_3O_4 (nMag) by addition of a strong base to a solution of Fe^{2+} and Fe^{3+} salts in water. This method is very simple, inexpensive and produces highly crystalline nMag. The general size of nMag produced by co-precipitation is in the 15 to 50 nm range and can be controlled by reaction conditions, however a large size distribution of nanoparticles is produced by this method. Aggregation of particles is also observed with aqueous methods.

The thermal decomposition method consists of the high temperature thermal decomposition of an iron-oleate complex derived from an iron precursor in the presence of surfactant in a high boiling point organic solvent under an inert atmosphere. For the many variations of this synthetic method many different solvents and surfactants are used. However, in most every method nMag is formed through the thermal decomposition of an iron-oleate complex to form highly crystalline nMag in the 5 to 40 nm range with a very small size distribution. The size of nMag produced is a function of reaction temperature, the iron to surfactant ratio, and the reaction time, and various methods are used that achieve good size control by manipulation of these parameters. The nMag synthesized by organic methods is soluble in organic solvents because the nMag is stabilized by a surfactant surface coating with the polar head group of the surfactant attached to and the hydrophobic tail extending away from the nMag (Figure 2.17). An example of a thermal decomposition method is shown in Figure 2.17.

---

[5]This content is available online at <http://cnx.org/content/m22167/1.6/>.
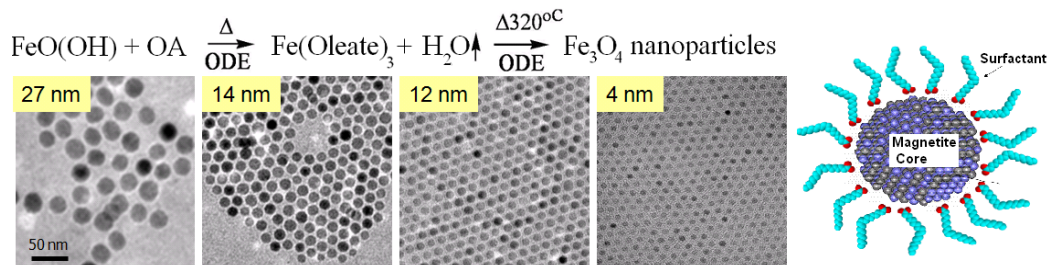
Figure 2.17: Top - The reaction equation for this method shows the iron precursor = iron oxo-hydrate, surfactant = oleic acid (OA), and solvent = 1-octadecene. The intermediate iron-oleate complex which thermally decomposes to nMag is formed upon heating the reaction mixture to the 320 °C reaction temperature. Bottom - TEM images showing size control by reaction time (time decreases left to right, constant molar ratio Fe:OA = 1:4 mol, and constant reaction temp T = 320 °C) and small size distribution of nMag. Right - Cartoon of surfactant coated nMag.

2.5.1 Bibliography

- A. Vioux, *Chem. Mater.* , 1997, **9** , 2292.

2.6 Kitchen Synthesis of Nanorust[6]

Kitchen Synthesis of Nanorust
J.T. Mayo, Courtney Payne, Lauren Harrison, Cafer Yavuz, Dr. Mary McHale, Professor Vicki Colvin
Objectives

- To perform a kitchen synthesis
- To obtain functional iron oxide nanocrystals that can be used for water purification of arsenic in Third World countries by using everyday items found in any kitchen.
- To appreciate the many forms of iron and the many uses of iron oxide nanocrystals.
- To appreciate the advanced analytical instruments that are used in the continuing research of nanotechnology.
- Remember: Thinking simple saves money and lives.

Grading
Your grade will be determined according to the following:

- Pre-lab (10%)
- Lab Report Form (80%)
- TA points (10%)

Background

---

[6]This content is available online at <http://cnx.org/content/m20813/1.3/>.
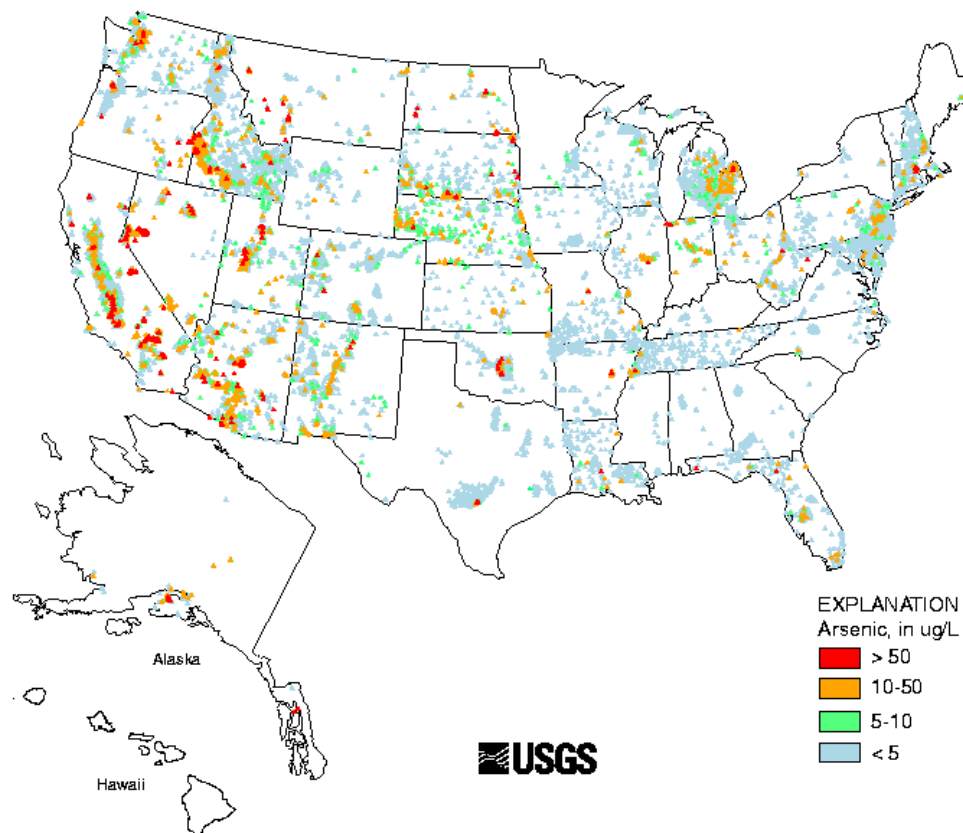
Figure 2.18

Having clean drinking water is one of the most fundamental necessities of life. There are many different forms of possible contamination, but among the most well-studied and problematic inorganic contaminants is arsenic. Arsenic is one of the oldest known carcinogens. In 1999, the US National Academy of Sciences reported that arsenic can cause bladder, lung and skin cancer, and possibly cause liver and kidney cancer. The physical symptoms of arsenic poisoning include: extreme fatigue, nausea, vomiting, partial paralysis, and reproductive damage.[7] Arsenic is naturally occurring in water due to its abundance in certain types of rocks, but it can have anthropogenic origins as well.

Arsenic can be found all over the world, but is currently a particular problem in Third World countries due to the costly nature of water purification. It is especially abundant in Bangladesh, but arsenic has also been found in the ground water of Argentina, Chile, India, Mexico, Taiwan and Thailand. Additionally, closer to home, most states in the western US have levels of arsenic concentrations of greater than 10 parts per billion (10 ppb). This was not a cause for concern until the Environmental Protection Agency (EPA) in 2006 lowered the maximum allowable level of arsenic from 50 ppb to 10 ppb. In 2001, approximately 13 million Americans were drinking water that had elevated levels of arsenic in the water.[8]

Previous methods for arsenic removal have included: manganese greensand columns that have been pretreated with dilute acid, coagulation/microfiltration, iron oxide based filtration, and activated alumina. The "Arsenic Removal Using Bottom Ash" or "ARUBA" method, invented by Ashok Gadgil of the Lawrence Berkeley National Laboratory, involves coating the surface of the contaminants with bottom ash and ferric

---

[7]**National Research Council.**_Arsenic in drinking water._ Washington, DC, National Academy Press, 1999.
[8]http://www.epa.gov/safewater/arsenic/index.html

hydroxide. Bottom ash is sterile waste material from coal-fired power plants which would make the cost of remediation about 0.5 cents per kg ARUBA of which generally 4-5 grams of ARUBA is needed for 1 liter of water, initially containing 400 ppb arsenic.

Nanomagnetite synthesis for arsenic removal has been hailed as Forbes: 'Top 5 Nanotech Breakthroughs of 2006' and Esquire listed it as 'Six Ideas That Will Change the World' in 2007. Basically, the technique entails forming iron oxide nanocrystals that possess very unique and size-dependent characteristics for environmental remediation of arsenic contaminated water.

Introduction
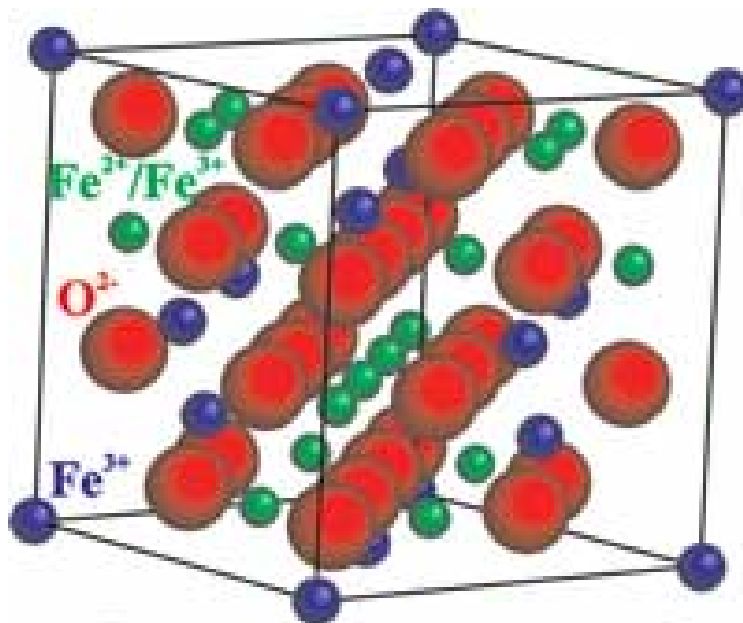
Figure 2.19

Both iron oxide nanocrystals: Fe_3O_4 (magnetite) and Fe_2O_3 (maghemite, as it is a cross between MAGnetite and HEMatite) are ferrimagnetic materials which means they can behave as permanent magnets. Additionally, those oxides below 10 nanometers in diameter, exhibit superparamagnetic properties and are used as MRI contrast agents.

Remember that last semester, you prepared a solution of magnetite ferrofluid by mixing iron(II) chloride and iron(III) chloride in the presence of tetramethylammonium hydroxide.

Magnetite is the most magnetic of all the naturally occurring minerals on Earth and has shown a lot of promise in environmental remediation as it efficiently removes As(III) and As(V) from water, this efficiency of the removal increases ∼200 times when the magnetite particle size decreases from 300 to 12 nm. Since arsenic contaminated drinking water is a major problem around the world, using magnetite as a sorbent shows a great deal of promise.

Additionally, Fe(II) compounds have been used to oxidize organic contaminants such as trichloroethylene (TCE), while inorganic contaminants such as arsenic, lead and uranium are separated out of solution. Between 10 and 20 nanometers, the contaminants can be removed from water via handheld magnets, which is an important consideration in purifying water in the Third World, where power is not a standard commodity.

We will produce nanocrystalline and functional iron oxides following a green approach by using everyday

items and equipment found in kitchens worldwide. The nanocrystalline and functional oxides are produced by thermal decomposition of the iron-precursors in order to form highly uniform, isolatable nanocrystals of tunable size. The iron precursors will decompose into iron oxides in organic solvents (thermally stable non-polar solvents, aka fatty acids such as oleic acid) at temperatures in excess of 200ºC; the presence of amphiphilic stabilizers, in this case fatty acids derived from soap, limits the growth of crystalline products which are either magnetite, maghemite, or mixtures of both phases.

The beauty of this method lies in the ability to use inexpensive iron sources, such as rust, to form iron carboxylate intermediates, that when scaled to the gram level effectively produces a relatively low cost method for removal of arsenic from contaminated water (see Table 1).

Rust is a mixture of iron hydroxides, oxides, and in some cases even zero-valent iron, but is as effective as FeOOH used in any laboratory method. The fatty acid used in conventional methods is oleic acid, an unsaturated 18 carbon fatty acid. It can be replaced by many cooking oils that can be processed to create a homemade soap through saponification, by the addition of a base such as lye. The soap is allowed to cure for a few days and then dissolved in a weak acid, such as vinegar. The organic layer of the liquid can be collected and used without further processing. The "fatty acid mixture" or FAM is an impure fatty acid whose exact composition depends on the starting edible oil. Olive oil contains the most oleic acid; coconut oils contain more lineolic acid. For this lab, the FAM is derived from vegetable oil, a standard starting reactant.

Pure lab chemicals		Everyday chemicals	
Chemical	Price per kg	Chemical	Price per kg
FeOOH	$ 778.00	Rust	$ 0.20*
Oleic acid	$ 20.60	Edible oil (coconut oil)	$ 0.25
1-octadecene	$ 24.75	Crystal drain opener (NaOH)	$ 1.24
		Vinegar	$ 0.65
Magnetite Nanocrystals	**$ 2,624.00**	Magnetite Nanocrystals	**$ 21.7**

Table 2.1

Table 1. Cost comparison of the materials needed for a FAM/rust synthesis of magnetite nanocrystals with a conventional laboratory synthesis. Most of the savings results from the reduction in cost of the iron source. *Cost of the rust is an estimate.

In the kitchen synthesis, the black product that forms can be separated from the solution by simply using a handheld magnet rather than the expensive and large centrifuges used in a conventional laboratory setting.

Experimental Procedure

Caution!! While all of the following chemicals and utensils can be found in a kitchen, this procedure is potentially dangerous (even the soap is caustic). Gloves and goggles must be worn at all times!!

Materials

- vegetable oil
- lye or 100% NaOH drain opener
- wooden spoon
- glass bowl
- 5% vinegar
- cooking pot
- hot plate
- turkey baster or plastic pipette
- rust

Part 1: Soap making process
   This step requires a week of advanced preparation and has been done for you

1. In a crystallization dish or a similar container, weigh 100 g. of the liquid oil (if not liquid gently melt it and keep as melted).
2. In a 50 mL vial (or a cup) weigh 15 g. of crystal drain opener (or caustic soda, or sodium hydroxide, or potash).
3. Add 30 mL of tap water and shake (or stir) until all solid is dissolved (CAUTION: solution gets hot!). While still warm pour it into the liquid oil.
4. Stir with a spoon (or a magnetic stir bar) for about **15 minutes** (or until tracing occurs – tracing is the visible tracks of stirring).
5. Let it sit open to air in a hood (or ventilated area) to dry and cure for a few weeks. If a shorter time span is allotted, the soap can be dried in an oven. To help the drying process, the excess oil can be decanted after 48 hours. Use caution when decanting the soap as there may be excess unreacted NaOH present.

Part 2: Oleic acid from soap with commercial vinegar

1. Grate the soap given to you and weigh it. You should have approximately 30 grams. If you have extra soap, do not discard it; give it back to your TA.
2. Check the vinegar's acidity (i.e. 5%).
3. Use 1 mL of acid for every gram of soap (i.e. 30 mL of acid, 600 mL of commercial vinegar with 5% acidity).
4. Combine the vinegar and soap in a cooking pot.
5. Heat on med-high and stir with a wooden spoon until all of the chunks are dissolved (light boiling is preferred). – This takes 15 to 30 minutes.

Caution!! This must be done a hood or other well-ventilated area!!

1. Turn off the heating and cool the solution down.
2. Pour your solution into the 1L beaker provided. You should see two layers separating from each other.
3. Separate the top yellowish layer using a turkey baster or plastic pipette into a 50 mL beaker. Make sure you get as much of the organic layer that as you can out of the vinegar/acid mixture.
4. Separate the organic layer off again into another 50 mL beaker so that you are left with only the organic layer. This is your fatty acid mixture (FAM)
5. Thoroughly clean your cooking pot in the sink with soap and water.

Part 3: Magnetite nanocrystals from rust and fatty acids

1. Carefully measure 0.5 grams of rust. Do not discard excess rust; put it back in the stock container.
2. Mix the rust with the fatty acid mixture in the cooking pot.
3. Cover the top of the container with a loose cap for proper ventilation. The reaction smokes and steams. This method produces 50-90 nm nanocrystals.
4. Start heating and timing. The rust should be heated for roughly 1 hour, until the solution is dark black with little or no smoking. Remember to continue stirring at regular intervals. Do not heat the oil to the point of popping and spattering. Adjust the heat as necessary so that the solution only steams and smokes.

 Caution!! This must be done a hood or other well-ventilated area!!

1. If your rust solution looks like it might dry out, notify your TA immediately and they will provide you with extra oleic acid to complete your reaction. DO NOT LET YOUR RUST DRY ONTO THE FRYING PAN!!!!!!!

2. Once the rust solution appears dark black and little to no smoke is being produced, pour the nanorust solution into a 50 mL beaker.
3. Hold a magnet to the side of the beaker and observe what happens. Hold the magnet to the beaker for several minutes.
4. Clean the cooking pot thoroughly again with soap and water. If there is any black or burnt crusting, this needs to be scrubbed away.

2.7 Semiconductor Nanoparticles[9]

The most studied non-oxide semiconductors are cadmium chalcogenides (CdE, with E = sulfide, selenide and telluride). CdE nanocrystals were probably the first material used to demonstrate quantum size effects corresponding to a change in the electronic structure with size, i.e., the increase of the band gap energy with the decrease in size of particles (Figure 2.20). These semiconductors nanocrystals are commonly synthesized by thermal decomposition of an organometallic precursor dissolved in an anhydrous solvent containing the source of chalcogenide and a stabilizing material (polymer or capping ligand). Stabilizing molecules bound to the surface of particles control their growth and prevent particle aggregation.

Figure 2.20: Picture of cadmium selenide (CdSe) quantum dots, dissolved in toluene, fluorescing brightly, as they are exposed to an ultraviolet lamp, in three noticeable different colors (blue ∼481 nm, green ∼520 nm, and orange ∼612 nm) due to the quantum dots' bandgap (and thus the wavelength of emitted light) depends strongly on the particle size; the smaller the dot, the shorter the emitted wavelength of light. The "blue" quantum dots have the smallest particle size, the "green" dots are slightly larger, and the "orange" dots are the largest.

Although cadmium chalcogenides are the most studies semiconducting nanoparticles, the methodology for the formation of semiconducting nanoparticles was first demonstrated independently for InP and GaAs, e.g., (2.3). This method has been adapted for a range of semiconductor nanoparticles.

$$InCl_3 + P(SiMe_3)_3 \rightarrow InP + 3\, Me_3SiCl$$

(2.3)

In the case of CdE, dimethylcadmium $Cd(CH_3)_2$ is used as a cadmium source and bis(trimethylsilyl)sulfide, $(Me_3Si)_2S$, trioctylphosphine selenide or telluride (TOPSe, TOPTe) serve as sources of selenide in trioctylphosphine oxide (TOPO) used as solvent and capping molecule. The mixture is heated at 230-260

---

[9]This content is available online at <http://cnx.org/content/m22374/1.4/>.

°C over a few hours while modulating the temperature in response to changes in the size distribution as estimated from the absorption spectra of aliquots removed at regular intervals. These particles, capped with TOP/TOPO molecules, are non-aggregated (Figure 2.21) and easily dispersible in organic solvents forming optically clear dispersions. When similar syntheses are performed in the presence of surfactant, strongly anisotropic nanoparticles are obtained, e.g., rod-shaped CdSe nanoparticles can be obtained.
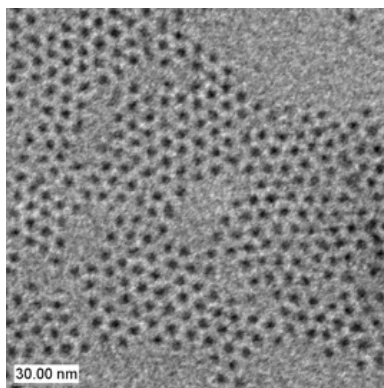
Figure 2.21: TEM image of CdSe nanoparticles.

Because $Cd(CH_3)_2$ is extremely toxic, pyrophoric and explosive at elevated temperature, other Cd sources have been used. CdO appears to be an interesting precursor. CdO powder dissolves in TOPO and HPA or TDPA (tetradecylphosphonic acid) at about 300 °C giving a colorless homogeneous solution. By introducing selenium or tellurium dissolved in TOP, nanocrystals grow to the desired size.

Nanorods of CdSe or CdTe can also be produced by using a greater initial concentration of cadmium as compared to reactions for nanoparticles. This approach has been successfully applied for synthesis of numerous other metal chalcogenides including ZnS, ZnSe, and $Zn_{1-x}Cd_xS$. Similar procedures enable the formation of MnS, PdS, NiS, Cu_2S nanoparticles, nano rods, and nano disks.

2.7.1 Bibliography

- C. R. Berry, *Phys. Rev.*, 1967, **161**, 848.
- M. D. Healy, P. E. Laibinis, P. D. Stupik, and A. R. Barron, *J. Chem. Soc., Chem. Commun.*, 1989, 359.
- L. Manna, E. C. Scher, and A. P. Alivisatos, *J. Am. Chem. Soc.*, 2000, **122**, 12700.
- C. B. Murray, D. J. Norris, and M. G. Bawendi, *J. Am. Chem. Soc.*, 1993, **115**, 8706.
- Z. A. Peng and X. Peng, *J. Am. Chem. Soc.*, 2002, **12**, 3343.
- R. L. Wells, C. G. Pitt, A. T. McPhail, A. P. Purdy, S. R. B. Shafieezad, and Hallock *Chem. Mater.*, 1989, **1**, 4.
- X. Zong, Y. Feng, W. Knoll, and H. Man, *J. Am. Chem. Soc.*, 2003, **125**, 13559.

2.8 Silver Nanoparticles: A Case Study in Cutting Edge Research[10]

Alvin Orbaek, Mallam Phillips, Dr. Mary McHale, Prof. Andrew Barron,

---

[10]This content is available online at <http://cnx.org/content/m19597/1.11/>.

2.8.1 Objective

To gain an insight into nanotechnology, what it is and how it can be useful, using silver nanoparticles as an example. We will look at what exactly nanoparticles are, see how they are made, and how they can be characterized.

The characterization technique involves Ultra-Violet and Visible spectroscopy, so we will look briefly into the interaction of the nanoparticles and light, which will hopefully help you gain an appreciation for one of the special aspects of nanotechnology.

When making the nanoparticles we will do a time study allowing us to graph the spectroscopic response - which will show the nature of the particle as it grows, i.e., ripens. We can use some data to calculate the size of the nanoparticle at the beginning and at the end of our experiment.

2.8.2 Background

2.8.2.1 What is nanotechnology?

Nano is the ancient Greek word for dwarf. In scientific terms it has been used to identify length scales that are one billionth of a unit. This is typically a meter and so you often here things that are nanometers in size. In terms of nanotechnology it has been defined as anything that has a unique property or function resulting from the size of the artifact being in the nano regime, and that the size regime is between 0.1 and 100 nm. This size range is rather broad; encompassing simple molecules to more complicated molecules like enzymes. However, these items can be looked at from many points of view, from a chemist that considers molecules, to that of an engineer that would look at how each of the molecules interacts in the bigger system and creates new materials from these building blocks. For this reason there are many disciplines that are interested in the study of nanotechnology such as Chemistry, Physics, Engineering, Biological sciences, Material Sciences, Computer Science and many more besides. For this reason nanotechnology is not a strict discipline and many people use their skills and backgrounds from other areas to contribute to research in this particular field.

2.8.2.2 Why care about nanotechnology?

There are many effects that occur at the nanoscale that we do not notice on a larger macro scale. Most of nature actually works at the nanoscale, and by understanding the forces that are at work using knowledge from chemistry, physics and engineering one can better understand the working of organic life. Enzymes are very large molecules that are too large to consider in terms of chemistry alone, other effects come into play In order to understand the full picture we need to borrow from physics and computer modeling to gain a better understand of what is happening.

There are many effects that occur at the nanoscale that we do not notice on a larger macro scale. Most of nature actually works at the nanoscale, and by understanding the forces that are at work using knowledge from chemistry, physics and engineering one can better understand the working of organic life. Enzymes are very large molecules that are too large to consider in terms of chemistry alone, other effects come into play In order to understand the full picture we need to borrow from physics and computer modeling to gain a better understand of what is happening.

When we cross from the small scale as in molecules and atoms, to the large scale that we see with our own eyes, we travel through the nanoscale. In that scale we go from quantum physics to classical physics and a lot of very interesting effects can be used to our benefit, and actually nanoparticles are an excellent example of this. Just by virtue of their size they are able to absorb four times more light than is even shone on them! This is very different from the bulk material, it is difficult to understand in one sitting, but let's just say that there is a coupling between the light energy and the matter of the nanoparticles that is best explained through quantum mechanics, but we won't go into that now.

When you make something very large, there is lots of room for error, the more parts you have in a system the more chances there are that some of those parts can be faulty. However when you make something in the nanoscale you have far less parts in the system and each part has to be virtually perfect. Material

scientists are concerned with the defects that are created in materials, because these are the parts that cause a material to break down often and stop functioning correctly. As you get into the nanoscale there are less defects and you get enhanced effects from the purer material, that don't occur on the larger scale. One example of this is carbon nanotubes, by virtue of there shape and size they are 6 times lighter than steel, but almost 100 times stronger. There is great potential for using these in new materials in the future that are ultra lightweight and extremely strong.

When we make things with modern technology we have for centuries been using a top down approach, and this brings us down to a fine limit but not as fine as that on which nature works. Nanotechnology is more about understanding the fundamental forces in nature by physics, and seeing their interaction through chemistry, and then making something larger from our engineering skills. And we can always take examples from biology that has been doing this for far longer than we have. So really what we do is take a bottom up approach, so that we can create large materials that we can use, that has every part of the interaction tailored all the way from how the atoms interact and how the molecules are formed and bonded together to make building blocks for new materials and applications. This bottom up approach is a change in the way things have been done and for this reason nanotechnology is a very potent discipline, with an immense capacity for expansion.

In all we have only really begun to scratch the surface of what could be possible when we create things using nanotechnology, and we should be aware of this because nanotechnology is finding its way into every corner of life, from health studies, medicine, robotics, materials and maybe even food and many many more.

2.8.2.3 What are nanoparticles and how are they made?

A simple way of seeing this is by imagining tennis balls that are squeezed down to a few billionths of a meter. The particles are rounded because they try to minimize the surface energy as much as possible; any edges will make things more energetic since typically nature follows the path of least resistance the particles tend to form colloids, or spheres with as few edges as possible. It is possible though, to direct the growth of nanoparticles into various shapes such as cubes, and tetrahedrons. We will concern ourselves with only colloidal nanoparticles for the moment.

The nanoparticles have a large surface area compared with the total volume. The surface area to volume ratio is interesting because chemical reactions typically occur on surfaces, so nanoparticles that have a high surface to energy ratio can be used in many interesting ways, such as in catalysis. One teaspoon of nanoparticles might weigh only 200 mg, but because of their shape and the large amount of surface area the tea spoon could have the same surface area as a whole football field! This gives them huge potential and potency compared to the bulk material. Imagine laying out a football field with a thin layer of silver, think how much silver that would need, and then compare that with the amount that is in the spoon! This high surface area to volume ratio is one of the most important properties about nanoparticles.

With all that surface area and the energy that exists, the nanoparticles need to be held together 'somehow'. That is where the furry parts of the tennis ball come into play. Imagine them as small molecules that hold on to the surface of the particle and stop it from breaking up under its own energy. It is like a tree whose roots can prevent soil erosion because the soil is bonded to the root in the ground. The chemical we use in this lab is mercaptosuccinic acid, and this helps to hold the nanoparticles in shape by bonding to the surface of the particles.

There are a few basic points to remember about making nanoparticles:

1) You need a nucleation point, a place for the metal (silver in this case) to start bonding to one another and start growing into a larger particle. For this you often need some ingredient that can break down a metal salt, in this case silver nitrate, which is accomplished by using sodium borohydride. This reduces the silver nitrate into silver ions that are free then to bond with each other.

2) You need some mechanism to keep the particles at the nanoscale and stop them from ripping and growing into something much larger, this is accomplished using the capping agent mentioned earlier (mercaptosuccinic acid). A great deal of cutting edge research revolves around varying the capping agent in order to control the size of your nanoparticles and tailor them for specific tasks. But not only can you change the size of particles in this way, you can also change the shapes.

2.8.2.4 Why silver nanoparticles?

Silver is a very easily oxidized material; it has been used already commercially for its anti-microbial properties from athletic wear to sterilizing water. It has a very interesting interaction with light due to a dielectric constant that makes the light response occur in the visible regime. Notably silver is one of the only metals that can be tailored to respond across the full visible spectrum.

Their light interaction can then be used in various fields such as photonics where new materials can be made to transport light in a similar fashion to the optical cables that we use now, but with a higher yield. These waveguides act like wires and could be made smaller and lighter than present day wires, but carry more light.

Another use of this light interaction can be used for imaging in biological systems, where the nanoparticles can be used as vectors to carry drugs to specific sights because of specific capping agents being used, and the internal core can be used to image the delivery and ensure the cargo is delivered correctly to the correct location in the body. One group at Rice that is working on this exciting research is the Barron lab (http://python.rice.edu/∼arb/Barron.html[11]).

2.8.3 TA Demonstration on the Hydrophobicity of Silver

Adapted from George Lisensky's procedure that demonstrates the hydrophobicity of silver based on the Tollen's test and the ability of self-assembly of thiol monolayers (SAM) on gold surfaces:

Essentially your TA will coat silver with a monolayer of octadecanethiol, effectively producing a non-polar surface and causing water that is dropped onto this surface to bead up.

Once your TA has placed a clean microscope slide in a Petri dish. Your TA will place 8 small drops (or 4 large drops) of a 0.5 M solution on the microscope slide (Figure 2.22).

---

[11]http://python.rice.edu/∼arb/Barron.html
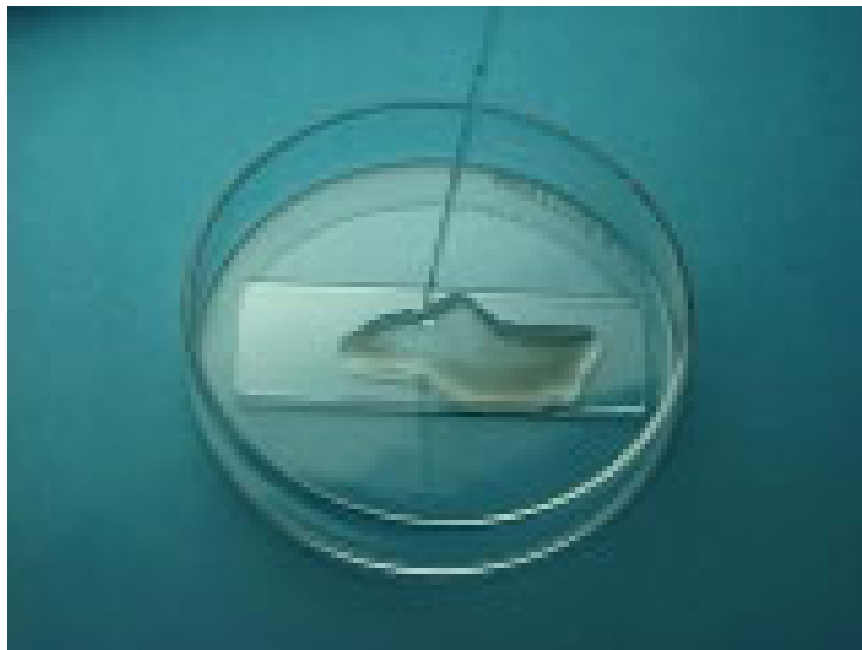
Figure 2.22: Image of a glucose solution beading on a glass slide.

Then your TA will add 25 small drops (or 12 large drops) of an active silver ion[12] solution (made by adding concentrated ammonia drop wise to 10 mL of 0.1 M silver nitrate solution until the initial precipitate just dissolves., followed by adding 5 mL of 0.8 M KOH solution; a dark precipitate will form (Figure 2.23). Add more ammonia drop wise until the precipitate just redissolves. This "active silver" solution has to be used within an hour of preparation. CAUTION: To avoid the formation of explosive silver nitride, discard any remaining active solution by washing down the drain with plenty of water) to the glucose solution and gently agitate to mix the solution.

---

[12]http://mrsec.wisc.edu/Edetc/nanolab/Agthiol/#materials2#materials2

Figure 2.23: Image of the preparation of the silver layer seen as a dark precipitate.

After waiting several minutes while the solution darkens and a grayish precipitate forms, a silver mirror is also forming on the slide, though it may be obscured by the precipitate c.f., Tollen's reagent. Your TA will use water from a wash bottle to wash off the precipitate and reveal the silver mirror (Figure 2.24) being careful to avoid contact with the solution since it will stain their hands.

Figure 2.24: Image showing the silver mirror formed on the glass slide.

Your TA will remove the slide from the Petri dish ensuring that he/she does not touch the silver solution, and rinse the silver mirror with water. How attracted are the water drops to the surface? (Like attracts like.) Do water drops on silver spread out or bead up?

The contact angle is between the side of a drop and the slide. Is the contact angle wide (small attraction to the slide) or narrow (large attraction to the slide)?

Your TA will wait for the surface to appear dry. (For faster drying we will use a hair dryer.) Cover the silver with a few drops of a long chain alkanethiol solution[13] , octadecanethiol, in ethanol (add a small amount of octadecanethiol, to 20 mL of ethanol. When finished, dispose of this solution by adding about 5 mL of household bleach. Let stand for several minutes then wash solution down the sink).

After the ethanol has evaporated, your TA will now have an alkanethiol monolayer with the sulfur atoms bound to the silver and the hydrocarbon tails pointing away. Your TA has effectively coated the surface with hydrocarbons.

How attracted are the water drops to the surface? (Like attracts like.)

Do water drops on the monolayer coated surface spread out or bead up?

Is the contact angle greater or less than before the alkanethiol was added?

Is the water attracted more to the plain glass, to the silver, or to the alkanethiol monolayer-coated silver?

2.8.4 Experimental Procedure no1 - ripening of silver nanoparticle

Solutions of silver nitrate (250 mg to 500 mL) and mercaptosuccinic acid (405 mg to 500 mL) have ALL been previously prepared for you. This can be gathered from the glass bottles situated in the lab.

---

[13]http://mrsec.wisc.edu/Edetc/nanolab/Agthiol/#materials3#materials3

1. Find and open the microlab program. Ensure that the accompanying box has power and is turned on, and that it is connected to the laptop via the USB plug. Once everything is connected and you double clock the microlab.exe file, a box will open in front of you.

2. In the tab labeled "New" you will find the icon for the "Spectrophotometer", please double click this.

3. This brings up the program that we will use, at which point you should take a reading of a blank sample, this is done by filling a vial with DI water and placing in the appropriate slot, and covering with the film case. When the blank sample is in place, click the button "Read Blank". This will a generate a series of data points that you can see.

4. Please take note to read from the Absorbance tab, this is the third option on the top right.

5. In a beaker gather 50 mL of silver nitrate solution; use the photo spectrometer to take an absorbance measurement of the silver solution on its own. To do this place twenty drops (approx 1 mL) into the glass vial provided, and dilute to the top with DI water. Shake the vial twice to ensure the solution is homogenous. Record the UV-Vis spectrum.

6. Place the 50 mL silver solution into the Erlenmeyer flask and start stirring, your TA will have the stir bars.

7. Complete the same process as above but this time uses 50 mL of the solution of mercaptosuccinic acid. Please make sure to rinse out the glass vial thoroughly. Take a spectrum using the photo spectrometer of the MSA solution.

8. Now place the 50 mL of MSA solution into the Erlenmeyer with the silver that you are already stirring vigorously – this means stirring at such a rate that you can see a vortex created.

9. Take a spectrum of the solution that is currently stirring, this should include the MSA and silver. You should notice, similar to DI water, and the MSA and silver on their own, that there is no response in absorbance of either of the chemicals when analyzed combined that would indicate that the nanoparticles have not been formed yet, but all the final ingredients are already there. This is why we need to add the sodium borohydride, as this will break the silver nitrate up so the silver can bind with the sulfur atom in the MSA molecule and the silver ions can start bunching up and the nanoparticles can begin to form.

10. Make the sodium borohydride solution by diluting 300 mg with DI water to 100 mL using a volumetric flask. From the equation of the chemical, $NaBH_4$, and upon the addition of water did you notice anything occurring, what happened in the reactions? (Did it change color, consistency, did gas evolve) what could have caused this? Sodium borohydride is highly hygroscopic, that means it reacts very readily with water, and the water in the atmosphere (especially in Houston) could have caused the salt to harden – this means you may have to coax the salt a little with some prodding using the spatula – without breaking the spatula!

11. To the solution of silver nitrate and mercaptosuccinic acid that is stirring place a few drops of the sodium borohydride solution, note the color change, then place some more sodium borohydride and note the color change again. What do you think is happening here, and why is the colors changing? What were the colors of the solution? Stop adding sodium borohydride when the color has reached a steady state and is not changing anymore. If you add too much sodium borohydride the products could come out of solution.

12. When you have a steady dark, black coffee color, you have added sufficient sodium borohydride Immediately take 20 drops of your Ag nanoparticle solution and place into the glass vial; make sure it is diluted down to a slightly sandy color by the addition of DI water. Place the filled vial into the slot and acquire spectroscopic data in the same manner as before, this will be your "time = 0" run – now what is different this time, compared with the last spectra you aquired? And how has this occurred?

13. Continue to repeat this process of taking 20 drops of your Ag nanoparticle solution and dilute in a vial and take spectroscopic data every 5 minutes for a total of 50 minutes,

14. When you are finished completing the experimental runs, then you can export the data so that it can be graphed in Excel.

15. Go to File, then scroll down to 'Export Data as.' and then select "Comma separated values'. This generates a file ending in .csv that can be later opened and used in Microsoft Excel; please take note

where the file was saved.

16. Use excel to graph each of the data sets on the same graph. Complete an Area graph, with 3D visualization to graph the ripening process. You should notice some of the intensity changing from the first data set until the last – why do you think this is happening?

17. Using Excel again take the data from the first profile and data from the profile with the tallest peak. Graph each one separately. This is to demonstrate how the nanoparticles ripen over time. So you can see there is some movement in the system and it can take several hours before the entire system reaches some equilibrium. Note: You will not see the trough that we showed you in the PowerPoint as MicroLab does not go down to 310 nm, which is why we are posting data so that you can calculate the full width half maximum..

18. You have now successfully made some silver nanoparticels! Congratulations.

19. Finally plot a graph from the data posted online in order to calculate the diameter of the nanoparticels once you have extrapolated the full width half maximum (FWHM), using the equation:

$D = 230/(FWHM-50)$. For help on getting the FWHM use Figure 2.25.
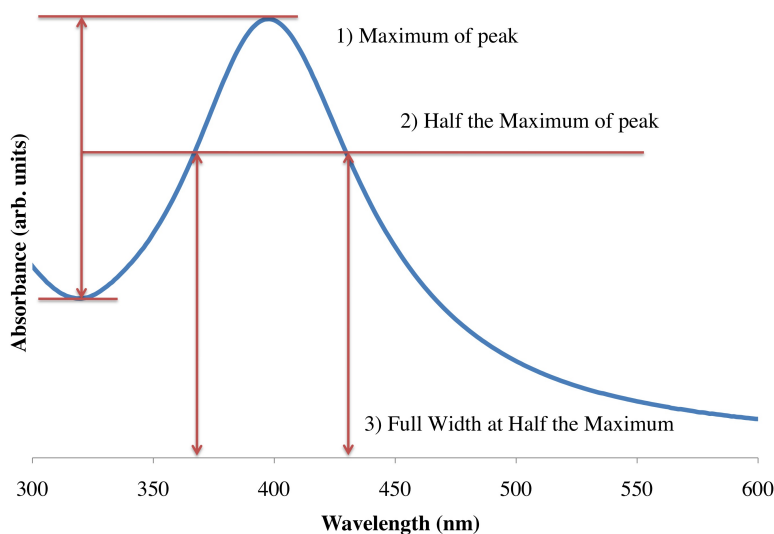
Figure 2.25: A plot demonstrating the three steps to obtain the FWHM from a graph of the UV-vis spectrum for the silver nanoparticles.

2.8.5 Experimental procedure no2 - lasers and colloids

When the nanoparticles form they are able to scatter huge amounts of light. As atoms the silver will not scatter any light, but when it is made into the form of nanoparticles the light scattering is possible to see using a simple laser light. Large chunks of silver cannot be soluble in water but it in the nanoparticle form it can be. We can use the laser pointers to see when the nanoparticles are forming.

During the first reaction you can see how sodium citrate takes a long time to create nanoparticles, at the beginning the laser does not shine through the solution. But over a period of about 20 minutes you will be able to see the nanoparticle form by using the laser light. When the nanoparticles have formed you will be able to see the laser run through the solution.

When you make the nanoparticles with sodium borohydride now, it is so strong it will make nanoparticles much faster. This reaction only takes about 2 minutes to occur.

Aim

1. To synthesize silver nanoparticles using two different reducing agents
2. To see the difference in the rates of reaction between the two reducing agents
3. To use laser pointers to determine when the nanoparticles form and hence, to see which reducing agent works faster

Sodium Citrate

1. In a glass vessel gather 75 mL of silver nitrate solution. Put this on a hot plate and place a stir bar inside it. Start heating the solution with a medium setting, start the stir bar so that a small vortex occurs in the solution.
2. After a period of five minutes when the solution is getting warmer, place 2 mL of tri sodium citrate into the solution that is warming on the heat place. Make sure to add the sodium citrate drop wise. This will take about two minutes to do.
3. Now use a laser pointer to see if any nanoparticles have formed.
4. Over a period of 20 minutes you should notice a change in color that occurs because of the formation of the silver nanoparticles. Continuously use the laser pointer to look for the formation of nanoparticles.
5. Turn off the hot plates and take the glass away from the heat.
6. When the solution has cooled to room temperature place the waste in the waste container.

Sodium Borohydride

1. In a glass vessel gather 75 mL of silver nitrate solution. Place a stir bar inside the reaction vessel and start stirring with a speed that creates a small vortex.
2. Gather 50 mL of mercaptosuccininc acid (MSA) and place this inside the same vessel as the silver nitrate that you have recently got.
3. Use the laser to light to see if there are any nanoparticles present.
4. Now get your TA to help distribute some sodium borohydride for you. This is a very reactive chemical and will loose strength over time. Your TA will place sodium borohydride in the reaction vessel.
5. While your TA is adding the sodium borohydride, check to see if any nanoparticles are forming by using the laser light.
6. When the reaction is completed place the materials in the waste container.
7. Clean all your glassware.

Conclusion

Nanoparticles are an exciting and emerging technology. There is much to learn about how to use these new structures. It is a delicate and complex process to learn how to make thing so small, but as you have discovered today, it is not impossible to do. The detection of nanoparticles can be easily achieved with the use of a hand held laser pointer. This is due to the extremely large scattering cross section that nanoparticles have.

2.8.6 Additional Information

We use light to see things around us, that light has a certain size, or wavelength. And if something is smaller than light, we cannot use the light to see it directly, so we have to use things with smaller wavelengths. Let's use an example, consider a hand of a certain size, and some hieroglyphics on a wall(er?). With very large

hands the details in the wall are difficult to make out, but still you can note that they are there. But when you use smaller and smaller hands the details become easier to make out. It's the same kind of idea when using the light. For us as human beings it is not usually a problem in our everyday lives, the size of the light is much smaller than the artifacts we deal with as we move around. But when looking at smaller and smaller things as in the nanoscale, we can't use visible light because the light passes right over the objects normally, and it's as if they don't exist.

One trick around this is to use shorter wavelengths of light, like using X-rays at the hospital to image brakes and fractures of the skeletal system. And in nanotechnology what we often use are electrons, Because the wavelength of the electrons are far smaller than the object we are looking at, we can get a good picture of what is going on at the nanoscale. There are two main instruments to do this: the TEM (transmission electron microscope), and the SEM (scanning electron microscope). In the same way that the X-rays at the hospital pass through the skin but not the bones, the TEM accelerates electrons through materials, and depending on the type and size of the material the electrons either pass through or not. And we get a black and white image of our system at the nanoscale. In Figure 2.26 you see a picture of the type of silver nanoparticles that you made in the lab, this was taken with a TEM in Dell Butcher Hall here at Rice. The dense silver particles don't allow the transmission of the electrons, and we get a black and white picture of the nanoparticles. This has been calibrated and can be used to tell us the size of the particles; they are around 10 nm on average.
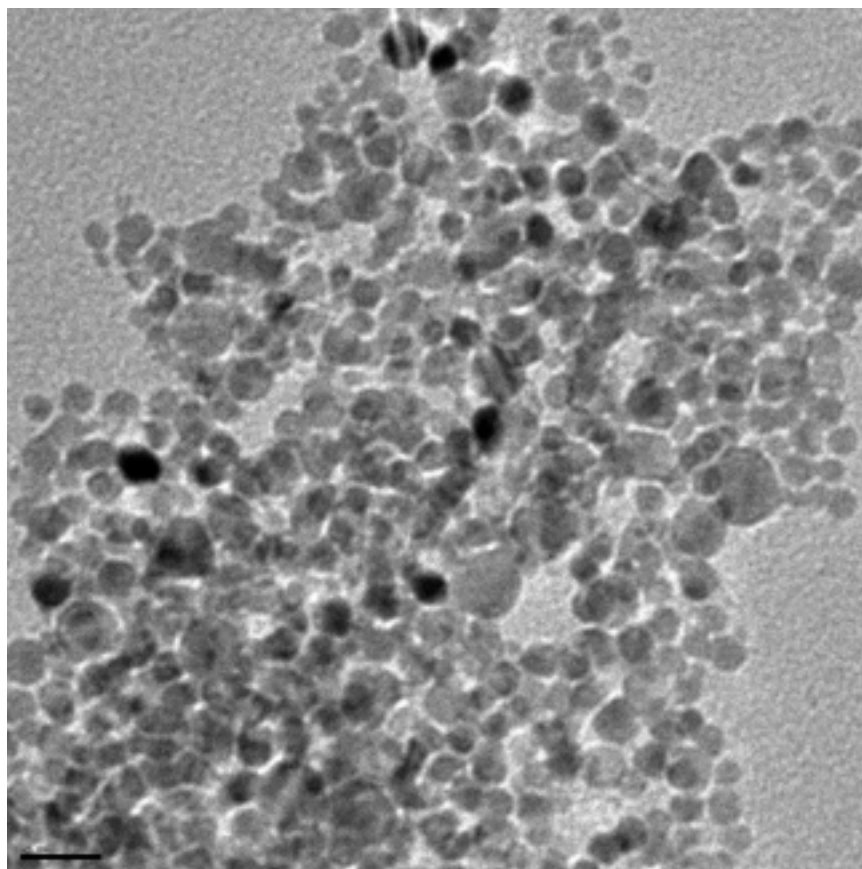
Figure 2.26: TEM image of silver nanoparticles, scale bar is 20 nm.

But when electrons pass through the material it is not always a clean break, some of the energy can be imparted on the materials and so it won't pass all the way through. This can cause a secondary effect that depends on the material that is being imaged, and this is essentially how the SEM works. Instead of electrons passing through like in the X-rays in the hospital, the materials you image have a reaction to the bombardment of electrons in the electron beam. In Figure 2.27 you see a bunch of larger silver nanoparticles that have been imaged using an SEM here in Dell Butcher Hall at Rice University.
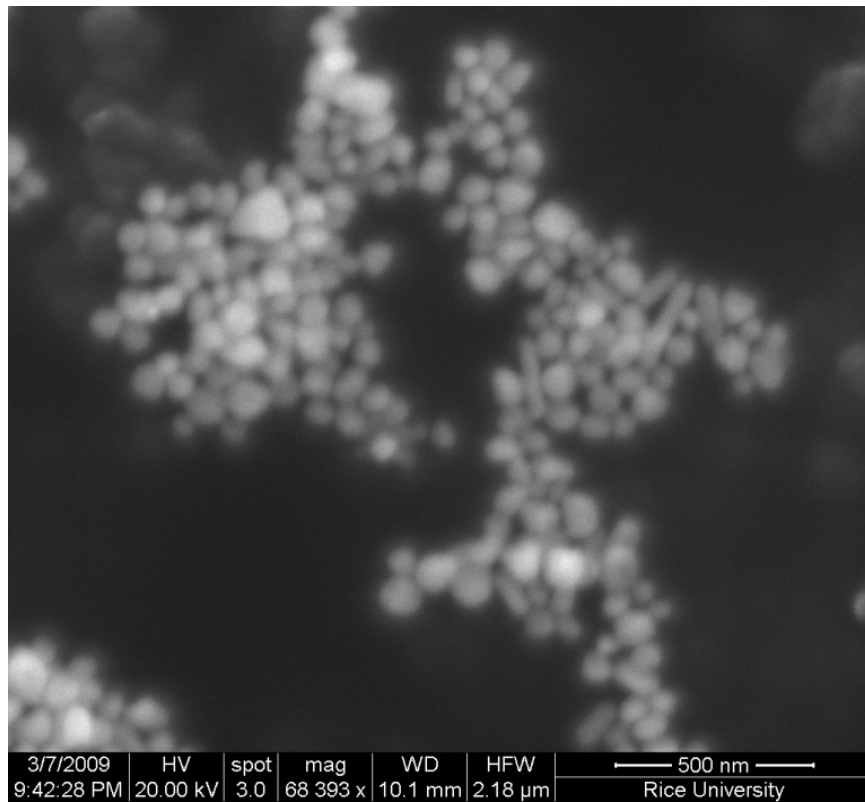
Figure 2.27: SEM image of larger silver nanoparticles, scale bar is 500 nm.